

1 **A Multiscale Model of Partial Melts 1: Effective** 2 **Equations**

G. Simpson

3 Department of Mathematics, University of Toronto, Toronto, ON M5S 2E4,
4 Canada.

M. Spiegelman

5 Department of Applied Physics and Applied Mathematics, Columbia
6 University, New York, New York, USA. Lamont-Doherty Earth Observatory,
7 Palisades, NY 10964, USA.

M. I. Weinstein

8 Department of Applied Physics and Applied Mathematics, Columbia
9 University, New York, New York, USA.

G. Simpson, Department of Mathematics, University of Toronto, Toronto, ON M5S 2E4,
Canada. (simpson@math.toronto.edu)

M. Spiegelman, Department of Applied Physics and Applied Mathematics, Columbia Univer-
sity, New York, NY 10027, USA. Lamont-Doherty Earth Observatory, Palisades, NY 10964, USA.
(mspieg@ldeo.columbia.edu)

M. I. Weinstein, Department of Applied Physics and Applied Mathematics, Columbia Univer-
sity, 200 Mudd, New York, NY 10027, USA. (miw2103@columbia.edu)

10 **Abstract.** Developing accurate and tractable mathematical models for
11 partially molten systems is critical for understanding the dynamics of mag-
12 matic plate boundaries as well as the geochemical evolution of the planet.
13 Because these systems include interacting fluid and solid phases, develop-
14 ing such models can be challenging. The composite material of melt and solid
15 may have emergent properties, such as permeability and compressibility, that
16 are absent in the phase alone. Previous work by several authors have used
17 multiphase flow theory to derive macroscopic equations based on conserva-
18 tion principals and assumptions about interphase forces and interactions. Here
19 we present a complementary approach using homogenization, a multiple scale
20 theory. Our point of departure is a model of the microstructure, assumed to
21 possess an arbitrary, but periodic, microscopic geometry of interpenetrat-
22 ing melt and matrix. At this scale, incompressible Stokes flow is assumed to
23 govern both phases, with appropriate interface conditions.

24 Homogenization systematically leads to macroscopic equations for the melt
25 and matrix velocities, as well as the bulk parameters, permeability and bulk
26 viscosity, without requiring ad-hoc closures for interphase forces. We show
27 that homogenization can lead to a range of macroscopic models depending
28 on the relative contrast in melt and solid properties such as viscosity or ve-
29 locity. In particular, we identify a regime that is in good agreement with pre-
30 vious formulations, without including their attendant assumptions. Thus this
31 work serves as independent verification of these models. In addition, homog-

32 enization provides a consistent machinery for computing consistent macro-
33 scopic constitutive relations such as permeability and bulk viscosity that are
34 consistent with a given microstructure. These relations are explored numer-
35 ically in a companion paper.

1. Introduction

36 Developing quantitative models of partially molten regions in the Earth is critical for
37 understanding the dynamics of magmatic plate boundaries such as mid-ocean ridges and
38 subduction zones, as well as for providing a better integration of geochemistry and geo-
39 physics. Beginning in the mid 1980’s there have been multiple derivations of macro-
40 scopic equations for magma dynamics that describe the flow of a low-viscosity fluid in
41 a viscously deformable, permeable solid matrix [*McKenzie*, 1984; *Scott and Stevenson*,
42 1984, 1986; *Fowler*, 1985, 1989; *Spiegelman*, 1993; *Stevenson and Scott*, 1991; *Bercovici*
43 *et al.*, 2001a, b; *Ricard et al.*, 2001; *Hier-Majumder et al.*, 2006; *Bercovici and Ricard*,
44 2005, 2003; *Ricard and Bercovici*, 2003; *Ricard*, 2007]. The details and specific processes
45 included, vary slightly among these model systems but all are derived using the methods
46 of multiphase flow [e.g. *Drew and Segel*, 1971; *Drew*, 1971, 1983].

47 Multiphase flow techniques are well formulated in many texts, including *Drew and*
48 *Passman* [1999]; *Brennen* [2005]. Typically, the two-phase medium is examined at a
49 macroscopic scale, much larger than the pore or grain scale, and one attempts to develop
50 effective media equations based on conservation of mass, momentum, and energy. This
51 approach is reasonably straightforward and has proven useful in applications, notably di-
52 lute disperse flows. However, they have two fundamental sources of uncertainty. First,
53 an appropriate “interphase force” must be posited. There is often a tremendous range
54 of mathematically valid choices for this force with little to constrain it beyond physical
55 intuition and experimental validation. Second, the macroscopic equations derived for the
56 partial melt problem include critical constitutive relations, such as permeability, bulk vis-

57 cosity or effective shear viscosity. These should depend on the microscopic distribution of
58 melt and matrix, information that is often lost in the multiphase flow approach. Multi-
59 phase flow does not naturally determine these relationships. As with the interphase force,
60 these closures require estimates from scalings, numerical simulations, and experiments.

61 In this and a companion paper [*Simpson et al.*, 2008b], we present a complementary
62 method for deriving effective macroscopic equations using the methods of homogenization
63 theory. Rather than assume macroscopic equations and then seek closures for constitutive
64 relations, we assume microscopic equations and derive the macroscopic equations. This
65 is done by a multiple scale expansion, which encodes both fine and coarse length scales
66 into the field variables. As in all multiple scale methods, the equations are matched at
67 each order of the small parameter and solved successively. For a useful introduction to
68 homogenization with applications see *Hornung* [1997]; *Torquato* [2002]. More rigorous
69 mathematical treatments are presented in *Bensoussan et al.* [1978]; *Sanchez-Palencia*
70 [1980]; *Cioranescu and Donato* [1999]; *Chechkin et al.* [2007]; *Pavliotis and Stuart* [2008].
71 Homogenization has been used extensively for flow in rigid and elastic porous media, but
72 we believe this is the first application to the magma dynamics problem which permits
73 viscous deformation of the matrix.

74 This strategy has several advantages with respect to multiphase flow methods. In partic-
75 ular, there is no under-constrained interphase force, as these effects are described precisely
76 by boundary conditions between the phases at the micro scale. Second, and perhaps more
77 importantly, it provides a mechanism for computing consistent macroscopic constitutive
78 relations for a given microscopic geometry. For the magma dynamics problem, it yields a
79 collection of auxiliary “cell problems” whose solutions determine the bulk viscosity, shear

viscosity, and permeability of the medium consistent with the micro-structure. We emphasize that these macroscopic effective quantities are not volume averages of microscopic quantities. Indeed, permeability and bulk viscosity are undefined at the grain scale, but they appear as macroscopic properties through homogenization. More generally, homogenization can extract tensor valued permeabilities and shear viscosities for anisotropic media. The methods presented are also adaptable to other fine scale rheologies and physics.

In this work, we specifically consider the simplest case of homogenization of the momentum equations for two coupled Stokes problems involving a high viscosity phase (the solid matrix) and a low viscosity fluid. This work is adapted from studies of sintering and partially molten metal alloys, [*Auriault et al.*, 1992; *Geindreau and Auriault*, 1999], which in turn is based on earlier work in poro-elastic media [e.g., *Auriault*, 1987, 1991a; *Auriault and Boutin*, 1992; *Mei and Auriault*, 1989; *Mei et al.*, 1996; *Auriault and Royer*, 2002]. For clarity, we only consider linear viscous behavior for the solid, as this may be appropriate for the diffusion creep regime [e.g., *Hirth and Kohlstedt*, 1995a]. This assumption considerably simplifies the analysis. Extensions to power-law materials are discussed in *Geindreau and Auriault* [1999].

We demonstrate that, depending on the choice of scalings, we can derive homogenized macroscopic equations for three different regimes, and identify a particular regime that is consistent with existing and commonly used formulations such as *McKenzie* [1984] and *Bercovici and Ricard* [2003]. This provides independent validation of these other systems. We also discuss the strengths and weaknesses of homogenization and identifies some open questions. We recognize that the derivation is somewhat technical but have attempted to

103 make the overall approach as accessible as possible with the hope that other researchers
104 will extend these methods to related problems (e.g., including surface energies and more
105 complex rheologies).

106 The second paper is more practical and provides specific computation of cell-problems
107 to calculate consistent permeabilities, bulk-viscosities and effective shear viscosities for
108 several simplified pore geometries. In particular we provide a derivation for the bulk
109 viscosity and demonstrate that, for a purely mechanical coupling of phases, it should scale
110 inversely with the porosity; a relationship we conjecture is insensitive to the specifics of
111 the microscopic geometry. Such an inverse relationship has been suggested before [e.g.
112 *Schmeling, 2000; Bercovici and Ricard, 2003*]; however, this is the first rigorous derivation
113 from the microscale. Further implications of these results are discussed in the second
114 paper.

115 *Simpson et al. [2008a, b]* are based on the PhD. thesis of G. Simpson, *Simpson [2008]*.

2. Problem Description

2.1. Macroscopic and Microscopic Domains

116 To begin the upscaling procedure, we must describe the spatial domains occupied by
117 each phase. We denote with symbol Ω the total macroscopic region of interest, containing
118 both the melt and the matrix, with a characteristic length scale L which might be an
119 observed macroscopic characteristic wavelength (e.g. 1 m–10 km). Initially, we assume
120 that within Ω the matrix has a periodic microstructure. A two-dimensional analog is
121 pictured in Figure 1. Ω , the bounded gray region, is tiled with a fluid filled pore network
122 of period ℓ . ℓ is a representative measure of length scale of the grains or pore distribution,

123 such as a statistical moment of the grain size distribution, and is much smaller than L .
 124 Notation for the domains is given in Table 1.

We form the first important dimensionless parameter, ϵ ,

$$\epsilon \equiv \frac{\ell}{L} \quad (1)$$

ϵ will play two important roles in what follows. First, all other dimensionless numbers and parameters will be expressed in powers of ϵ . Second, we will expand the dependent variables in powers in ϵ as in

$$\Phi = \Phi^{(0)} + \epsilon\Phi^{(1)} + \epsilon^2\Phi^{(2)} + \dots \quad (2)$$

125 Of course, real partially molten rocks are not a periodic medium. Pore structures similar
 126 to those expected in peridotite appear in Figure 3. Since it is crystalline, there is some
 127 regularity, but it is closer to a *random* medium. While only the periodic case is treated in
 128 this work, the random one is of interest and is also amenable to homogenization, *Torquato*
 129 [2002].

We divide our domain Ω from Figure 1 into three subregions:

Ω_f —The fluid portion of Ω .

Ω_s —The solid portion of Ω .

Γ —The interface between fluid and solid in Ω .

130 We shall write equations for the melt in Ω_f , equations for the matrix in Ω_s , and boundary
 131 conditions between the two along Γ .

132 We now introduce the notion of a cell. The cell, appearing in Figure 2 and denoted with
 133 the symbol Y , is a scaled, dimensionless, copy of the periodic microstructure of Figure 1.
 134 This is divided into a fluid region, Y_f , a solid region, Y_s , and an interface, γ . A simple

135 three-dimensional example of such a cell appears is displayed in Figure 4. The cell should
 136 be interpreted as a scaled representative elementary volume of the grain scale. It may be
 137 a single grain or a small ensemble of grains.

138 Although the connectedness of both phases is an important property, the particular
 139 microstructure of Y does not play a significant role in the form of macroscopic equations.
 140 Cell geometry does determine the magnitudes and forms of the constitutive relations
 141 appearing in the equations. This is discussed in the companion paper.

2.2. Grain Scale Equations

At the microscale, we assume both phases are incompressible, linearly viscous, isotropic fluids. The rheology for each phase is:

$$\boxed{\sigma = -pI + 2\mu e(\mathbf{v})} \quad (3)$$

where $e(\mathbf{v})$ is the strain-rate tensor,

$$\boxed{e(\mathbf{v}) = \frac{1}{2} (\nabla \mathbf{v} + (\nabla \mathbf{v})^T)} \quad (4)$$

Components may be accessed by index notation:

$$e_{ij}(\mathbf{v}) = \frac{1}{2} \left(\frac{\partial v_i}{\partial X_j} + \frac{\partial v_j}{\partial X_i} \right)$$

$$\sigma_{ij} = -p\delta_{ij} + 2\mu e_{ij}(\mathbf{v})$$

142 The variable \mathbf{X} appearing in these expressions denotes the dimensional spatial vari-
 143 able. The stress in Ω_s for the solid phase is σ^s , with pressure p^s and velocity \mathbf{v}^s . Similarly,
 144 the fluid has stress σ^f , pressure p^f , and velocity \mathbf{v}^f in Ω_f . The notation for the fields is
 145 given in Table 2.

At the pore scale, the Reynolds number is small; using the the values of Table 3, the value in the melt is $\lesssim O(10^{-5})$ and as low as $O(10^{-30})$ in the matrix. Therefore, we will

omit inertial terms in the conservation of momentum equations. Each phase satisfies the Stokes equations at the grain scale; the divergence of the stress of each phase balances the body forces. As we are interested in buoyancy driven flow, the forces $\mathbf{g}^s \equiv -\rho_s g \mathbf{e}_3$ and $\mathbf{g}^f \equiv -\rho_f g \mathbf{e}_3$ are included. The equations are:

$$\nabla \cdot \sigma^f + \mathbf{g}^f = 0 \quad \text{in } \Omega_f \qquad \nabla \cdot \sigma^s + \mathbf{g}^s = 0 \quad \text{in } \Omega_s \qquad (5a)$$

$$\nabla \cdot \mathbf{v}^f = 0 \quad \text{in } \Omega_f \qquad \nabla \cdot \mathbf{v}^s = 0 \quad \text{in } \Omega_s \qquad (5b)$$

Conditions at the interface between fluid and solid, Γ , are still needed. As both are viscous, we posit continuity of velocity and normal stress:

$$\mathbf{v}^s = \mathbf{v}^f, \quad \text{on } \Gamma \qquad (6a)$$

$$\sigma^s \cdot \mathbf{n} = \sigma^f \cdot \mathbf{n}, \quad \text{on } \Gamma \qquad (6b)$$

146 A Boussinesq approximation has been made by taking the velocities to be continuous
 147 as opposed to the momenta. These equations are exact in the sense that, subject to
 148 boundary conditions on the exterior of Ω , solving them would provide a full description
 149 of the behavior of the two-phase medium (although it would be impractical to solve such
 150 a system at the macroscopic scale of interest).

2.3. Scalings

Our effective equations emerge from multiple scale expansions of the dependent variables. The dimensional spatial variable \mathbf{X} specifies a position within either Ω_s or Ω_f . We introduce two dimensionless spatial scales, \mathbf{y} , the “fast” spatial scale, and \mathbf{x} , the “slow”

spatial scale. These relate to \mathbf{X} , and one another, as:

$$\mathbf{y} \equiv \mathbf{X}/\ell \tag{7a}$$

$$\mathbf{x} \equiv \mathbf{X}/L = \epsilon\mathbf{y} \tag{7b}$$

The expansion in (2) is now made more precise. All variables are assumed, initially, to have both fast and slow scale dependence:

$$\Phi(\mathbf{y}) = \Phi^{(0)}(\epsilon\mathbf{y}, \mathbf{y}) + \epsilon\Phi^{(1)}(\epsilon\mathbf{y}, \mathbf{y}) + \epsilon^2\Phi^{(2)}(\epsilon\mathbf{y}, \mathbf{y}) + \dots \tag{8}$$

151 Such an expansion captures grain scale detail in the second argument, while permitting
 152 slow, macroscopic variations in the first argument. As we take our domain to be peri-
 153 odically tiled with scaled copies of the cell Y , we assume $\Phi^{(j)}(\mathbf{x}, \mathbf{y})$ is \mathbf{y} -periodic at all
 154 orders of j . We seek equations that are only functions of \mathbf{x} ; these will be the effective
 155 macroscopic equations.

Before making series expansions in powers of ϵ , the equations must be scaled appropriately. In addition to ϵ , there are several other important dimensionless numbers. As motivation, let P^s, P^f, V^s, V^f be characteristic pressures and velocities for the solid and fluid phases. We write:

$$p^f = P^f \tilde{p}^f \qquad p^s = P^s \tilde{p}^s \tag{9}$$

$$\mathbf{v}^f = V^f \tilde{\mathbf{v}}^f \qquad \mathbf{v}^s = V^s \tilde{\mathbf{v}}^s \tag{10}$$

Tildes reflect that the variables are now dimensionless and $O(1)$. Using these definitions, we non-dimensionalize (5a). We are free to scale the equations to either the slow or fast length scale. In this work, we scale to the ℓ length, though this does not affect the results.

On the length scale ℓ , the force equations are:

$$\begin{aligned} \nabla_y \cdot \left[-\tilde{p}^f I + \left(\frac{\mu_f V^f}{P^f \ell} \right) 2\tilde{\mu}_f e_y(\tilde{\mathbf{v}}^f) \right] + \frac{\rho_f g \ell}{P^f} \tilde{\mathbf{g}}^f &= 0 \\ \nabla_y \cdot \left[-\tilde{p}^s I + \left(\frac{\mu_s V^s}{P^s \ell} \right) 2\tilde{\mu}_s e_y(\tilde{\mathbf{v}}^s) \right] + \frac{\rho_s g \ell}{P^s} \tilde{\mathbf{g}}^s &= 0 \end{aligned} \quad (11)$$

where e_y denotes the strain-rate tensor with velocity gradients taken with respect to the fast length scale y . This motivates defining four more dimensionless numbers:

$$\mathcal{Q}_\ell^f \equiv \frac{\mu_f V^f}{P^f \ell} \quad \mathcal{Q}_\ell^s \equiv \frac{\mu_s V^s}{P^s \ell} \quad (12)$$

$$\mathcal{R}_\ell^f \equiv \frac{\rho_f g \ell}{P^f} \quad \mathcal{R}_\ell^s \equiv \frac{\rho_s g \ell}{P^s} \quad (13)$$

The \mathcal{Q} 's measure the relative magnitudes of the viscous forces and the pressure gradients, while the \mathcal{R} 's measure the relative magnitudes of the body forces and the pressure gradients. The $\tilde{\mu}$'s and $\tilde{\mathbf{g}}$'s remain in the equations as $O(1)$ constants. Three other important parameters are the ratio of the viscosities of the two phases, the ratio of the velocities of the two phases, and the ratio of the pressures of the phases:

$$\mathcal{M} \equiv \frac{\mu_f}{\mu_s} \quad (14)$$

$$\mathcal{V} \equiv \frac{V^f}{V^s} \quad (15)$$

$$\mathcal{P} \equiv \frac{P^f}{P^s} \quad (16)$$

¹⁵⁶ A full list of dimensionless numbers is given in Table 4.

Starting with ϵ , \mathcal{V} , and \mathcal{M} , we estimate these parameters with the data in Table 3:

$$\mathcal{M} = O(10^{-21} - 10^{-14}) \quad (17)$$

$$\mathcal{V} = O(10^1 - 10^3) \quad (18)$$

$$\epsilon = O(10^{-7} - 10^{-2}) \quad (19)$$

For these values, $\mathcal{M} \ll \epsilon \ll \mathcal{V}$. Since we expand the equations in powers of ϵ , we relate all quantities to ϵ . A quantity Q is said to be $O(\epsilon^p)$ if

$$\epsilon^{p+1} \ll Q \ll \epsilon^{p-1} \tag{20}$$

In terms of ϵ , \mathcal{M} and \mathcal{V} are approximately:

$$\mathcal{M} = O(\epsilon^{11} - \epsilon^2) \tag{21}$$

$$\mathcal{V} = O(\epsilon^0 - \epsilon^{-2}) \tag{22}$$

157 We emphasize that this power of ϵ scale is less precise than a power of 10 scale. For
 158 example, \mathcal{V} might be $O(10^1)$, but if $\epsilon = O(10^{-4})$, we would say $\mathcal{V} = O(\epsilon^0 = 1)$ since
 159 $\mathcal{V} \ll \epsilon^{-1}$. Indeed, in one of the scaling regimes we consider, $\mathcal{V} = O(\epsilon^0 = 1)$.

To estimate the other parameters, we need estimates of the characteristic pressures. To do this, we first consider the forces on the matrix. At the macroscopic scale, the melt is $O(1\%)$ of the medium's volume. We thus argue that on this scale, the matrix is “close” to satisfying the Stokes equations; the pressure gradient, viscous forces, and gravity balance one another. On the large length scale L , the dimensionless form of (5a) is

$$\nabla_x \cdot \left[-\tilde{p}^s I + \left(\frac{\mu_s V^s}{P^s L} \right) 2\tilde{\mu}_s e_x(\tilde{\mathbf{v}}^s) \right] + \frac{\rho_s g L}{P^s} \tilde{\mathbf{g}}^s = 0. \tag{23}$$

Similar to Equation (11), we define

$$\mathcal{Q}_L^s \equiv \frac{\mu_s V^s}{P^s L} \tag{24}$$

$$\mathcal{R}_L^s \equiv \frac{\rho_s g L}{P^s} \tag{25}$$

For the terms to be in balance, $\mathcal{Q}_L^s = O(1)$ and $\mathcal{R}_L^s = O(1)$. Using (24–25) and the definition of ϵ , the fast length scale parameters are:

$$\mathcal{Q}_\ell^s = O(\epsilon^{-1}) \quad (26)$$

$$\mathcal{R}_\ell^s = O(\epsilon^1) \quad (27)$$

In the absence of direct pressure measurements, we assume the pressures are the same order,

$$\mathcal{P} = O(1 = \epsilon^0). \quad (28)$$

An argument for this is given in *Drew* [1983]. Briefly, since the velocities of interest are far less than the speed of sound, it would be difficult to support large pressure gradients across the phases without surface tension, a mechanism we do not include. We make an additional assumption that there are $O(1)$ non-hydrostatic pressures in both phases; if $p = p_{\text{hydro}} + p_{\text{non-hydro}}$ then

$$\left| \frac{p}{p_{\text{non-hydro}}} \right| = O(1 = \epsilon^0). \quad (29)$$

In the fluid, since $\rho_f/\rho_s = O(1)$, a consequence of $\mathcal{P} = O(1)$ is

$$\mathcal{R}_\ell^f = \frac{\rho_f g \ell}{P^f} = \frac{\rho_s g \ell}{P^s} \frac{\rho_f}{\rho_s} \frac{P^s}{P^f} = \mathcal{R}_\ell^s \frac{\rho_f}{\rho_s} \mathcal{P} = O(\epsilon^1) \quad (30)$$

The fluid's force ratio is

$$\mathcal{Q}_\ell^f = \frac{\mu_f V^f}{P^f \ell} = O(\mathcal{P} \mathcal{M} \mathcal{V} \mathcal{Q}_\ell^s) = O(\epsilon^{-1} \mathcal{M} \mathcal{V}) \quad (31)$$

and

$$\mathcal{Q}_L^f = \mathcal{M} \mathcal{V} \quad (32)$$

Therefore,

$$\mathcal{M}\mathcal{V} = O(\epsilon^{10} - \epsilon^1) \quad (33)$$

$$\mathcal{Q}_\ell^f = O(\epsilon^9 - \epsilon^0) \quad (34)$$

160 The choice of dimensionless parameters will lead to different expansions and effective
 161 equations. In the terminology of *Auriault* [1991a, b]; *Geindreau and Auriault* [1999];
 162 *Auriault et al.* [1992], we can derive one of several outcomes: *biphasic* media, *monophasic*
 163 media, and *non-homogenizable* media. In the biphasic case, the macroscopic description
 164 possesses a distinct velocity field for each phase. In the monophasic case *both* phases
 165 have the same velocity field and we have a single, hybrid, material. In both biphasic and
 166 monophasic models, there is only one pressure. The non-homogenizable case is explained
 167 in Appendix D.

From here on, we assume

$$\boxed{\mathcal{Q}_\ell^f = O\left(\frac{\mathcal{M}\mathcal{V}}{\epsilon}\right) = O(\epsilon)} \quad (35)$$

168 which implies that at the microscale, the ratio of viscous stresses to pressure in the liquid
 169 phase is $O(\epsilon)$. This includes two biphasic cases, $(\mathcal{M}, \mathcal{V}) = (O(\epsilon^2), O(1))$ and $(\mathcal{M}, \mathcal{V}) =$
 170 $(O(\epsilon^3), O(\epsilon^{-1}))$, and a related monophasic case. We discuss the significance of constraint
 171 (35) in Section 4.1.

2.4. Main Results

172 Before proceeding with the expansions, we state our main results. The dependent
 173 variables are \mathbf{V}^s , the leading order velocity in the matrix, P , the leading order (fluid)
 174 pressure, and \mathbf{V}^f , the leading order mean velocity in the fluid. Full notation is given in
 175 Table 5.

176 The following systems of equations are derived in Section 3 and Appendices A–C by mul-
 177 tiple scale expansions. They employ an additional assumption that the cell microstructure
 178 possesses certain symmetries which are discussed in Section 3.6 and Appendix E.

Biphasic-I: In the first biphasic case, $\mathcal{V} = O(1)$ and $\mathcal{M} = O(\epsilon^2)$, the leading order non-dimensional equations are:

$$0 = \bar{\rho}\mathbf{g} - \nabla P + \nabla \left[\left(\zeta_{\text{eff.}} - \frac{2}{3}\mu_s(1 - \phi) \right) \nabla \cdot \mathbf{V}^s \right] \quad (36a)$$

$$+ \nabla \cdot [2(1 - \phi)\mu_s e(\mathbf{V}^s)] + \nabla \cdot [2\eta_{\text{eff.}}^{lm} e_{lm}(\mathbf{V}^s)]$$

$$\phi(\mathbf{V}^f - \mathbf{V}^s) = -\frac{k_{\text{eff.}}}{\mu_f} (\nabla P - \mathbf{g}^f) \quad (36b)$$

$$\nabla \cdot [\phi\mathbf{V}^f + (1 - \phi)\mathbf{V}^s] = 0 \quad (36c)$$

179 Again, we emphasize that the assumption $\mathcal{V} = O(1 = \epsilon^0)$ does not imply that the melt and
 180 solid velocities are equal, simply that the ratio of the viscosities is of significantly different
 181 order than the ratio of the velocities. The lm terms are summed over all pairs of l and m .
 182 $k_{\text{eff.}}$ is a scalar permeability (and more generally a second order tensor), $\zeta_{\text{eff.}}$ is an effective
 183 scalar bulk viscosity, and for each pair of indices (l, m) , $\eta_{\text{eff.}}^{lm}$ is the anisotropic contribution
 184 to the effective shear viscosity, a second order tensor. These material properties, defined in
 185 terms of microscale “cell problems” have been simplified through the domain symmetries.
 186 Derivatives are taken with respect to the dimensionless macroscopic scale \mathbf{x} , which we
 187 have suppressed as a subscript for clarity. We note that the equations for the Biphasic-I
 188 scaling are in good agreement with previous formulations. The chief difference is the
 189 appearance $\eta_{\text{eff.}}$ term capturing the grain scale anisotropy, which is new.

Biphasic-II: In the second biphasic case, $\mathcal{V} = O(\epsilon^{-1})$ and $\mathcal{M} = O(\epsilon^3)$, the macroscopic system is:

$$0 = \bar{\rho}\mathbf{g} - \nabla P + \nabla \cdot \left[\left(\zeta_{\text{eff.}} - \frac{2}{3}\mu_s(1 - \phi) \right) \nabla \cdot \mathbf{V}^s \right] \quad (37a)$$

$$+ \nabla \cdot [2(1 - \phi)\mu_s e(\mathbf{V}^s)] + \nabla \cdot [2\eta_{\text{eff.}}^{lm} e_{lm}(\mathbf{V}^s)]$$

$$\phi \mathbf{V}^f = -\frac{k_{\text{eff.}}}{\mu_f} (\nabla P + \mathbf{g}^f) \quad (37b)$$

$$\nabla \cdot (\phi \mathbf{V}^f) = 0 \quad (37c)$$

$\zeta_{\text{eff.}}$, $\eta_{\text{eff.}}$, and $k_{\text{eff.}}$ are as above. The first equation is the same as (36a) from the Biphasic-I model. The differences of the other two equations from (36b – 36c) reflect that when the fluid velocity is sufficiently greater than the solid velocity and the viscosities are sufficiently different, the coupling between phases has weakened. In this scaling regime the two phases only communicate through the pressure gradient.

Monophasic: In the limit that the melt becomes disconnected, Biphasic-I limits to a monophasic system:

$$0 = \bar{\rho}\mathbf{g} - \nabla P + \nabla \cdot [2\mu_s(1 - \phi) e(\mathbf{V}^s) + 2\eta_{\text{eff.}}^{lm} e_{lm}(\mathbf{V}^s)] \quad (38a)$$

$$\nabla \cdot \mathbf{V}^s = 0 \quad (38b)$$

where $\eta_{\text{eff.}}$ is as above. This is an incompressible Stokes system modeling a composite material with an anisotropic viscosity.

3. Detailed Expansions and Matching Orders

This section and Appendices A–B provide the detailed derivation and expansions required to derive the Biphasic-I model summarized in Section 2.4. The other two models are derived in Appendix C. This material is admittedly technical but we want to provide sufficient information to offer a road map for related studies.

We begin by writing our equations in dimensionless form. For the scaling regimes we study, the dimensionless forms of the force equations, (11), the incompressibility equations, (5b), and the boundary conditions, (6a) and (6b), are:

$$\nabla_y \cdot [-\tilde{p}^s I + 2\epsilon^{-1} \tilde{\mu}_s e_y(\tilde{\mathbf{v}}^s)] + \epsilon \tilde{\mathbf{g}}^s = 0 \quad (39a)$$

$$\nabla_y \cdot [-\tilde{p}^f I + 2\epsilon^1 \tilde{\mu}_f e_y(\tilde{\mathbf{v}}^f)] + \epsilon \tilde{\mathbf{g}}^f = 0 \quad (39b)$$

$$\nabla_y \cdot \tilde{\mathbf{v}}^s = 0 \quad (39c)$$

$$\nabla_y \cdot \tilde{\mathbf{v}}^f = 0 \quad (39d)$$

$$[-\tilde{p}^s I + 2\epsilon^{-1} \tilde{\mu}_s e_y(\tilde{\mathbf{v}}^s)] \cdot \mathbf{n} = [-\tilde{p}^f I + 2\epsilon^1 \tilde{\mu}_f e_y(\tilde{\mathbf{v}}^f)] \cdot \mathbf{n} \quad (39e)$$

$$\tilde{\mathbf{v}}^s = \mathcal{V} \tilde{\mathbf{v}}^f \quad (39f)$$

All dependent variables are functions of both \mathbf{x} and \mathbf{y} . Periodicity in \mathbf{y} is imposed to capture the periodicity of the microstructure. Derivatives act on both arguments,

$$\boxed{\frac{\partial}{\partial y_i} \mapsto \frac{\partial}{\partial y_i} + \epsilon \frac{\partial}{\partial x_i}} \quad (40)$$

Analogously, divergence, gradient, and strain rate operators become:

$$\nabla_y \cdot \mapsto \nabla_y \cdot + \epsilon \nabla_x \cdot \quad (41a)$$

$$\nabla_y \mapsto \nabla_y + \epsilon \nabla_x \quad (41b)$$

$$e_y \mapsto e_y + \epsilon e_x \quad (41c)$$

3.1. Hierarchy of Equations

Expanding all variables using Eq. (8) and applying the two scale derivatives, we arrive at two hierarchies of equations, one for each phase, which can be solved successively.

Details of these expansions are given in Appendix A. For the matrix, each iterate is:

$$O(\epsilon^n) : \quad \nabla_y \cdot \sigma^{s(n)} + \nabla_x \cdot \sigma^{s(n-1)} + \delta_{n,1} \mathbf{g}^s = 0 \quad \text{in } Y_s \quad (42a)$$

$$O(\epsilon^{n+1}) : \quad \nabla_y \cdot \mathbf{v}^{s(n+1)} + \nabla_x \cdot \mathbf{v}^{s(n)} = 0 \quad \text{in } Y_s \quad (42b)$$

$$O(\epsilon^n) : \quad \sigma^{s(n)} \cdot \mathbf{n} = \sigma^{f(n)} \cdot \mathbf{n} \quad \text{on } \gamma \quad (42c)$$

$$\sigma^{s(n)} \equiv -p^{s(n)} I + 2\mu_s [e_x(\mathbf{v}^{s(n)}) + e_y(\mathbf{v}^{s(n+1)})] \quad (42d)$$

201 where $\delta_{n,1}$ is the Kronecker delta, such that gravity only acts at order $n = 1$. Gravity does
 202 not participate in the earlier iterates. Treating $\sigma^{s(n-1)}$ and $\mathbf{v}^{s(n)}$ as known, the equations
 203 can be interpreted as an inhomogeneous Stokes system for $\mathbf{v}^{s(n+1)}$ and $p^{s(n)}$. The first
 204 iterate of this system is at $n = -1$, and we set $\sigma^{s(-2)} = \mathbf{v}^{s(-1)} = \sigma^{f(-1)} = p^{s(-1)} = 0$.

We note that the above equations can be interpreted at each order as a linear system in the spirit of the linear algebra problem $\mathbf{A}\vec{x} = \vec{b}$. As with all such problems, there is a solvability condition which must be satisfied. For our system, the constraint can be interpreted as follows: to be solvable at order n , the integrated surface stress on the solid exerted by the fluid, must match the integrated force felt within in the solid,

$$\int_{\gamma} \sigma^{f(n)} \cdot \mathbf{n} dS = - \int_{Y_s} (\nabla_x \cdot \sigma^{s(n-1)} + \delta_{n,1} \mathbf{g}^s) dy. \quad (43)$$

205 The enforcement of (43) separates scales and steers us to the macroscopic system. This
 206 condition can be derived by integrating (42a) over Y_s , invoking the divergence theorem
 207 on the $\nabla_y \cdot \sigma^{s(n)}$ term, and applying boundary condition (42c).

Complementing the equations for the matrix is a hierarchy of equations for the melt phase:

$$O(\epsilon^{n+1}) : \quad \nabla_y \cdot \sigma^{f(n+1)} + \nabla_x \cdot \sigma^{f(n)} + \delta_{n,1} \mathbf{g}^f = 0 \quad \text{in } Y_f \quad (44a)$$

$$O(\epsilon^n) : \quad \nabla_y \cdot \mathbf{v}^{f(n)} + \nabla_x \cdot \mathbf{v}^{f(n-1)} = 0 \quad \text{in } Y_f \quad (44b)$$

$$O(\epsilon^n) : \quad \mathbf{v}^{f(n)} = \begin{cases} \mathbf{v}^{s(n)} & \text{on } \gamma \text{ if } \mathcal{V} = O(1), \\ \mathbf{v}^{s(n-1)} & \text{on } \gamma \text{ if } \mathcal{V} = O(\epsilon^{-1}). \end{cases} \quad (44c)$$

$$\sigma^{f(n)} \equiv -p^{f(n)} I + 2\mu_f (e_y(\mathbf{v}^{f(n-1)}) + e_x(\mathbf{v}^{f(n-2)})) \quad (44d)$$

208 As in the solid case, we treat lower order terms, $\sigma^{f(n-1)}$ and $\mathbf{v}^{f(n-2)}$ as known, then solve
 209 for pressure $p^{f(n)}$ and velocity $\mathbf{v}^{f(n-1)}$. The first iterate of this system is at $n = -1$, and
 210 we set $\sigma^{f(-1)} = \mathbf{v}^{f(-1)} = \mathbf{v}^{f(-2)} = \mathbf{v}^{s(-1)} = \mathbf{v}^{s(-2)} = 0$.

Again, there is a solvability condition. At each order, the flow of the solid at the boundary must balance the dilation or compaction of the fluid:

$$\int_{Y_f} \nabla_x \cdot \mathbf{v}^{f(n)} d\mathbf{y} = \begin{cases} - \int_{\gamma} \mathbf{v}^{s(n)} \cdot \mathbf{n} dS & \text{if } \mathcal{V} = O(1) \\ - \int_{\gamma} \mathbf{v}^{s(n-1)} \cdot \mathbf{n} dS & \text{if } \mathcal{V} = O(\epsilon^{-1}) \end{cases} \quad (45)$$

211 This can be derived by integrating (44b) over Y_f , invoking the divergence theorem on the
 212 $\nabla_y \cdot \mathbf{v}^{f(n)}$ term, and applying boundary condition (44c). Both solvability conditions (43)
 213 and (45) will be essential for developing macroscopic effective media equations.

3.2. Leading Order Equations

The leading order equations are the same in the three scaling regimes we examine. From (42a), (42b), (42c), and (44a), the leading equations are:

$$O(\epsilon^{-1}) : \quad \nabla_{\mathbf{y}} \cdot \boldsymbol{\sigma}^{s(-1)} = 0 \quad \text{in } Y_s \quad (46a)$$

$$O(\epsilon^0) : \quad \nabla_{\mathbf{y}} \cdot \mathbf{v}^{s(0)} = 0 \quad \text{in } Y_s \quad (46b)$$

$$O(\epsilon^0) : \quad \nabla_{\mathbf{y}} \cdot \boldsymbol{\sigma}^{f(0)} = 0 \quad \text{in } Y_f \quad (46c)$$

$$O(\epsilon^{-1}) : \quad \boldsymbol{\sigma}^{s(-1)} \cdot \mathbf{n} = 0 \quad \text{on } \gamma \quad (46d)$$

214 These equations can be solved analytically to show that the leading order matrix velocity
215 and melt pressure are independent of the fine scale.

To solve for the leading order solid velocity $\mathbf{v}^{s(0)}$, note that the solid stress is $\boldsymbol{\sigma}^{s(-1)} = 2\mu_s e_y(\mathbf{v}^{s(0)})$ from (42d) and multiply (46a) by $\mathbf{v}^{s(0)}$ and integrate by parts over Y_s ,

$$\begin{aligned} & \int_{Y_s} \partial_{y_j} v_i^{s(0)} \sigma_{ij}^{s(-1)} d\mathbf{y} \\ &= \int_{\gamma} v_i^{s(0)} \sigma_{ij}^{s(-1)} n_j dS - 2\mu_s \int_{Y_s} |e_y(\mathbf{v}^{s(0)})|^2 d\mathbf{y} = 0 \end{aligned}$$

Applying the boundary condition (46d), we obtain

$$\int_{Y_s} |e_y(\mathbf{v}^{s(0)})|^2 d\mathbf{y} = 0.$$

which implies that $\mathbf{v}^{s(0)}$ is constant in \mathbf{y} ,

$$\mathbf{v}^{s(0)} = \mathbf{v}^{s(0)}(\mathbf{x}) \quad (47)$$

216 $\mathbf{v}^{s(0)}$ automatically satisfies (46b).

Turning to the fluid, the fluid stress is given by (44d) as $\boldsymbol{\sigma}^{f(0)} = -p^{f(0)}I$, thus (46c) becomes,

$$\nabla_{\mathbf{y}} \cdot \boldsymbol{\sigma}^{f(0)} = \nabla_{\mathbf{y}} \cdot (-p^{f(0)}I) = -\nabla_{\mathbf{y}} p^{f(0)} = 0.$$

which implies,

$$p^{f(0)} = p^{f(0)}(\mathbf{x}). \quad (48)$$

3.3. Successive Orders in the Solid Phase

At the next order ($n = 0$) in (42a–42c),

$$O(\epsilon^0) : \quad \nabla_y \cdot \sigma^{s(0)} = 0 \quad \text{in } Y_s \quad (49a)$$

$$O(\epsilon^1) : \quad \nabla_x \cdot \mathbf{v}^{s(0)} + \nabla_y \cdot \mathbf{v}^{s(1)} = 0 \quad \text{in } Y_s \quad (49b)$$

$$O(\epsilon^0) : \quad \sigma^{s(0)} \cdot \mathbf{n} = \sigma^{f(0)} \cdot \mathbf{n} \quad \text{on } \gamma \quad (49c)$$

From (42d),

$$\sigma^{s(0)} \equiv -p^{s(0)}I + 2\mu_s (e_y(\mathbf{v}^{s(1)}) + e_x(\mathbf{v}^{s(0)}))$$

Solvability condition (43) on the stresses is satisfied because $p^{f(0)} = p^{f(0)}(\mathbf{x})$ yielding

$$\int_{\Gamma} (-p^{f(0)}I) \cdot \mathbf{n} = 0.$$

It is helpful to define the pressure difference between solid and fluid as $q = p^{s(0)} - p^{f(0)}$.

$\mathbf{v}^{s(1)}$ and q solve

$$\nabla_y \cdot (-qI + 2\mu_s e_y(\mathbf{v}^{s(1)})) = 0 \quad \text{in } Y_s \quad (50a)$$

$$\nabla_y \cdot \mathbf{v}^{s(1)} = -\nabla_x \cdot \mathbf{v}^{s(0)} \quad \text{in } Y_s \quad (50b)$$

$$(-qI + 2\mu_s e_y(\mathbf{v}^{s(1)})) \cdot \mathbf{n} = (-2\mu_s e_x(\mathbf{v}^{s(0)})) \cdot \mathbf{n} \quad \text{on } \gamma \quad (50c)$$

This is an inhomogeneous Stokes problem with the forcing terms $\nabla_x \cdot \mathbf{v}^{s(0)}$ in (50b) and $2\mu_s e_x(\mathbf{v}^{s(0)}) \cdot \mathbf{n}$ in (50c); all forcing terms are independent of \mathbf{y} . Because the problem is linear, we can solve for each component of the forcing independently. The complete

solution is the superposition:

$$\mathbf{v}^{s(1)} = 2e_{x,lm}(\mathbf{v}^{s(0)})\bar{\chi}^{lm} - (\nabla_x \cdot \mathbf{v}^{s(0)})\bar{\xi} \quad (51)$$

$$q = p^{s(0)} - p^{f(0)} = 2\mu_s e_{x,lm}(\mathbf{v}^{s(0)})\pi^{lm} - \mu_s (\nabla_x \cdot \mathbf{v}^{s(0)})\zeta \quad (52)$$

217 Summation over lm is implied. For each ordered pair (l, m) , there is a velocity, $\bar{\chi}^{lm}$,
 218 and pressure, π^{lm} , contributed from the corresponding component of the surface stress on
 219 the solid, $2e_{x,lm}(\mathbf{v}^{s(0)})$. The velocity $\bar{\xi}$ and pressure ζ arise from the dilation/compaction
 220 forcing. $\bar{\chi}^{lm}$, π^{lm} , $\bar{\xi}$, and ζ are defined in Table 6 and full statements of the cell problems
 221 are given in Appendix B. These solve the aforementioned auxiliary, or cell, problems,
 222 which are Stokes boundary value problems posed on Y_s .

223 Cell problems may be interpreted as the unit response of the medium to a particular
 224 forcing. For generic three-dimensional cell geometries, the cell problems lack clear analytic
 225 solutions, and one must resort to numerical computation to understand them. In our
 226 second paper, we survey them numerically.

227 We make two observations on (52). First, it agrees with models that permit the pressures
 228 to be unequal, as in *Scott and Stevenson* [1984]; *Stevenson and Scott* [1991]; *Bercovici et al.*
 229 [2001a]; *Bercovici and Ricard* [2003]. It also makes clear that the question of whether
 230 there are one or two pressures in macroscopic models of partial melts is entirely semantic.
 231 There are two pressures, but to leading order each can be expressed in terms of the other.
 232 Second, it captures that part of any pressure jump is due to the macroscopic compaction
 233 of the matrix. Such a relation was also discussed in *Spiegelman et al.* [2007]; *Katz et al.*
 234 [2007].

3.4. Macroscopic Force Balance in the Matrix

235 Though we have solved for $\mathbf{v}^{s(1)}$, $p^{s(0)}$ in terms of $\mathbf{v}^{s(0)}$ and $p^{f(0)}$, we still do not have
 236 a macroscopic equation relating velocity and pressure. To find such an equation we go
 237 to the next order of equations for the matrix and use the solvability condition, (43), to
 238 constrain them. This constraint becomes our macroscopic equation; we do not actually
 239 solve for $\mathbf{v}^{s(2)}$ and $p^{s(1)}$.

At the next order of (42a–42c), the equations are:

$$O(\epsilon^1) : \quad \nabla_x \cdot \sigma^{s(0)} + \nabla_y \cdot \sigma^{s(1)} + \mathbf{g}^s = 0 \quad \text{in } Y_s \quad (53a)$$

$$O(\epsilon^2) : \quad \nabla_x \cdot \mathbf{v}^{s(1)} + \nabla_y \cdot \mathbf{v}^{s(2)} = 0 \quad \text{in } Y_s \quad (53b)$$

$$O(\epsilon^1) : \quad \sigma^{s(1)} \cdot \mathbf{n} = \sigma^{f(1)} \cdot \mathbf{n} \quad \text{on } \gamma \quad (53c)$$

$\sigma^{s(1)}$ is given by (42d):

$$\sigma^{s(1)} = -p^{s(1)} + 2\mu_s [e_x(\mathbf{v}^{s(1)}) + e_y(\mathbf{v}^{v(2)})] \quad (54)$$

According to our force matching solvability condition (43),

$$\int_{\gamma} \sigma^{f(1)} \cdot \mathbf{n} dS = - \int_{Y_s} (\nabla_x \cdot \sigma^{s(0)} + \mathbf{g}^s) d\mathbf{y} \quad (55)$$

By stress boundary condition (53c), $\sigma^{s(1)} \cdot \mathbf{n} = \sigma^{f(1)} \cdot \mathbf{n}$ on γ , so

$$\begin{aligned} \int_{Y_s} (\nabla_x \cdot \sigma^{s(0)} + \mathbf{g}^s) d\mathbf{y} &= - \int_{\gamma} \sigma^{f(1)} \cdot \mathbf{n} dS \\ &= \int_{Y_f} \nabla_y \cdot \sigma^{f(1)} d\mathbf{y} \end{aligned} \quad (56)$$

Using fluid momentum equation (44a), $\nabla_y \cdot \sigma^{f(1)} = -\nabla_x \cdot \sigma^{f(0)} - \mathbf{g}^f$ in Y_f , hence

$$\begin{aligned} \int_{Y_s} (\nabla_x \cdot \sigma^{s(0)}) d\mathbf{y} + \int_{Y_f} (\nabla_x \cdot \sigma^{f(0)}) d\mathbf{y} \\ + (1 - \phi) \mathbf{g}^s + \phi \mathbf{g}^f = 0 \end{aligned} \quad (57)$$

Commuting the integration and divergence operators,

$$\begin{aligned}
 & -\nabla_x [\langle p^{s(0)} \rangle_s + \langle p^{f(0)} \rangle_f] \\
 & + 2\mu_s \nabla_x \cdot [\langle e_x(\mathbf{v}^{s(0)}) \rangle_s + \langle e_y(\mathbf{v}^{s(1)}) \rangle_s] \\
 & + \bar{\rho} \mathbf{g} = 0
 \end{aligned} \tag{58}$$

where angle brackets $\langle \cdot \rangle_s$ denote volume averages over the solid domain Y_s (likewise $\langle \cdot \rangle_f$ over Y_f). If we substitute (51) and (52) for $p^{s(0)}$ and $\mathbf{v}^{s(1)}$, then

$$\begin{aligned}
 0 = & \bar{\rho} \mathbf{g} - \nabla_x p^{f(0)} \\
 & - \nabla_x \{ 2\mu_s e_{x,lm}(\mathbf{v}^{s(0)}) \langle \pi^{lm} \rangle_s - \mu_s \langle \zeta \rangle_s \nabla_x \cdot \mathbf{v}^{s(0)} \} \\
 & + 2\mu_s \nabla_x \cdot \{ (1 - \phi) e_x(\mathbf{v}^{s(0)}) + 2e_{x,lm}(\mathbf{v}^{s(0)}) \langle e_y(\bar{\chi}^{lm}) \rangle_s \} \\
 & - 2\mu_s \nabla_x \cdot \{ \langle e_y(\bar{\xi}) \rangle_s \nabla_x \cdot \mathbf{v}^{s(0)} \}
 \end{aligned} \tag{59}$$

240 We now have an equation for $\mathbf{v}^{s(0)}$ and $p^{f(0)}$, both functions of \mathbf{x} . Multiplying this equa-
 241 tion by P^s/L restores dimensions. *Again, we note that we did not solve (53a–53c).* (59) is
 242 merely the equation that must be satisfied for (53a–53c) to satisfy momentum compati-
 243 bility condition (43).

3.5. Macroscopic Force Balance in the Fluid

244 We now seek macroscopic equations for the melt. As in the case of the solid, we must
 245 iterate out to the second order correction and use the solvability condition to obtain a
 246 macroscopic equation.

We first solve for the first correction, obtaining $\mathbf{v}^{f(0)}$ and $p^{f(1)}$, and average them. From the hierarchy of fluid equations, (44a – 44d), the fluid equations at this order are

$$O(\epsilon^1) : \quad \nabla_x \cdot \sigma^{f(0)} + \nabla_y \cdot \sigma^{f(1)} + \mathbf{g}^f = 0 \quad \text{in } Y_f \tag{60}$$

$$O(\epsilon^0) : \quad \nabla_y \cdot \mathbf{v}^{f(0)} = 0 \quad \text{in } Y_f \tag{61}$$

with stress

$$\sigma^{f(1)} = -p^{f(1)}I + 2\mu_f e_y(\mathbf{v}^{f(0)})$$

and boundary conditions

$$\mathbf{v}^{f(0)} = \begin{cases} \mathbf{v}^{s(0)} & \text{on } \gamma \text{ if } \mathcal{V} = O(1) \\ 0 & \text{on } \gamma \text{ if } \mathcal{V} = O(\epsilon^{-1}) \end{cases} \quad (62)$$

247 One of the most relevant scaling regimes for magma migration is Biphasic-I with $\mathcal{V} =$
 248 $O(1)$ and $\mathcal{M} = O(\epsilon^2)$, summarized in Section 2.4. We derive it here. The two other
 249 systems, Biphasic-II and Monophasic, are similar and presented in Appendix C.

If we substitute the stresses $\sigma^{f(0)}$ and $\sigma^{f(1)}$ into (60 – 61), we have

$$\begin{aligned} -\nabla_x p^{f(0)} - \nabla_y p^{f(1)} + \mu_f \nabla_y^2 \mathbf{v}^{f(0)} + \mathbf{g}^f &= 0 \quad \text{in } Y_f \\ \nabla_y \cdot \mathbf{v}^{f(0)} &= 0 \quad \text{in } Y_f \end{aligned}$$

with boundary condition $\mathbf{v}^{f(0)} = \mathbf{v}^{s(0)}$ on γ . Recall that $p^{f(0)}$, $\mathbf{v}^{s(0)}$, and \mathbf{g}^f are interpreted as known, inhomogeneous, \mathbf{y} independent quantities forcing $\mathbf{v}^{f(0)}$ and $p^{f(1)}$. Since it is easier to solve a problem with homogeneous boundary conditions, we define $\mathbf{w} \equiv \mathbf{v}^{f(0)} - \mathbf{v}^{s(0)}$, simplifying the above equations into

$$-\nabla_y p^{f(1)} + \mu_f \nabla_y^2 \mathbf{w} = \nabla_x p^{f(0)} - \mathbf{g}^f \quad \text{in } Y_f \quad (63a)$$

$$\nabla_y \cdot \mathbf{w} = 0 \quad \text{in } Y_f \quad (63b)$$

$$\mathbf{w} = 0 \quad \text{on } \gamma \quad (63c)$$

250 This is the classic homogenization problem of flow in a rigid porous medium and leads to
 251 Darcy's Law. It is discussed in many of the cited texts on homogenization, particularly
 252 *Hornung* [1997].

The volume compatibility condition (45) is trivially satisfied since $\mathbf{w}|_\gamma = 0$,

$$0 = \int_{Y_f} (\nabla_y \cdot \mathbf{w}) d\mathbf{y} = \int_\gamma \mathbf{w} \cdot \mathbf{n} dS = 0.$$

As in the case of the solid phase, we solve (63a)–(64c) via cell problems, taking advantage of the linearity of the problem. We decompose the right hand side forcing terms in (63a) into \mathbf{e}_1 , \mathbf{e}_2 and \mathbf{e}_3 components, solving in each coordinate, then forming the superposition of the three to get the solution. Let q^i , \mathbf{k}^i be \mathbf{y} periodic functions solving:

$$-\nabla_y q^i + \nabla_y^2 \mathbf{k}^i = -\mathbf{e}_i \quad \text{in } Y_f \quad (64a)$$

$$\nabla_y \cdot \mathbf{k}^i = 0 \quad \text{in } Y_f \quad (64b)$$

$$\mathbf{k}^i = 0 \quad \text{on } \gamma \quad (64c)$$

\mathbf{e}_i is the unit vector in the i -th direction. These problems thus measure the unit response of the fluid to such a forcing. Using the solutions,

$$\mathbf{w} = -\frac{1}{\mu_f} \mathbf{k}^i \left(\partial_{x_i} p^{f(0)} - g_i^f \right) \quad (65)$$

$$p^{f(1)}(\mathbf{x}, \mathbf{y}) = -q^i \left(\partial_{x_i} p^{f(0)} - g_i^f \right) \quad (66)$$

Averaging over Y_f , we get the macroscopic equation for the fluid,

$$\langle \mathbf{v}^{f(0)} \rangle_f - \phi \mathbf{v}^{s(0)} = -\frac{\langle K \rangle_f}{\mu_f} (\nabla_x p^{f(0)} - \mathbf{g}^f) \quad (67)$$

This is Darcy's Law with buoyancy and in a moving frame. $\langle K \rangle_f$ is the permeability tensor. K is the matrix, or alternatively the second order tensor,

$$K = [\mathbf{k}^1 \quad \mathbf{k}^2 \quad \mathbf{k}^3] \quad (68)$$

and

$$\langle K \rangle_f = \left[\int_{Y_f} \mathbf{k}^1 d\mathbf{y} \quad \int_{Y_f} \mathbf{k}^2 d\mathbf{y} \quad \int_{Y_f} \mathbf{k}^3 d\mathbf{y} \right] \quad (69)$$

253 While the leading order solid velocity is \mathbf{y} -independent, the leading order fluid velocity
 254 remains sensitive to the fine scale. For a macroscopic description, it can only be defined
 255 as an average flux; this is the Darcy velocity of the fluid.

This is not yet a closed system. Advancing to the next order of (44a – 44c), we have

$$O(\epsilon^2) : \quad \nabla_x \cdot \sigma^{f(1)} + \nabla_y \cdot \sigma^{f(2)} = 0 \quad \text{in } Y_f \quad (70)$$

$$O(\epsilon^1) : \quad \nabla_x \cdot \mathbf{v}^{f(0)} + \nabla_y \cdot \mathbf{v}^{f(1)} = 0 \quad \text{in } Y_f \quad (71)$$

$$O(\epsilon^1) : \quad \mathbf{v}^{f(1)} = \mathbf{v}^{s(1)} \quad \text{on } \gamma \quad (72)$$

The solution must satisfy the volume compatibility condition (45),

$$\int_{Y_f} \nabla_x \cdot \mathbf{v}^{f(0)} = - \int_{\gamma} \mathbf{v}^{s(0)} \cdot \mathbf{n} dS = 0 \quad (73)$$

Combining this with (49b), we get

$$\nabla_x \cdot [\langle \mathbf{v}^{f(0)} \rangle_f + (1 - \phi) \mathbf{v}^{s(0)}] = 0 \quad (74)$$

256 This is a macroscopic volume compatibility condition. Equations (59), (67), and (74) now
 257 form a closed system. Dimensions may be restored to (67) by multiplying by V^f and (74)
 258 by V^f/L ; a factor of ℓ^2 will appear in front of $\langle K \rangle_f$, as expected.

3.6. Symmetry Simplifications

259 The macroscopic equations can be simplified if we assume that the cell geometry is
 260 symmetric with respect to both reflections about the principal axes and rigid rotations.
 261 Though this is a further idealization, the equations retain their essential features.

Under these two assumptions, (67) (for Biphasic I) and (C1) (for Biphasic II) are

$$\langle \mathbf{v}^{f(0)} \rangle_f - \phi \mathbf{v}^{s(0)} = - \frac{k_{\text{eff.}}}{\mu_f} (\nabla_x p^{f(0)} - \mathbf{g}^f) \quad (75)$$

$$\langle \mathbf{v}^{f(0)} \rangle_f = - \frac{k_{\text{eff.}}}{\mu_f} (\nabla_x p^{f(0)} - \mathbf{g}^f) \quad (76)$$

(59) becomes

$$0 = \bar{\rho}\mathbf{g} - \nabla_x p^{f(0)} + \nabla_x \left[\left(\zeta_{\text{eff.}} - \frac{2}{3}\mu_s(1 - \phi) \right) \nabla_x \cdot \mathbf{v}^{s(0)} \right] + \nabla_x \cdot \left[2(1 - \phi)\mu_s e_x(\mathbf{v}^{s(0)}) + 2\eta_{\text{eff.}}^{lm} e_{x,lm}(\mathbf{v}^{s(0)}) \right] \quad (77)$$

$k_{\text{eff.}}$, $\zeta_{\text{eff.}}$, and $\eta_{\text{eff.}}$ are defined in terms of the solutions of the cell problems:

$$k_{\text{eff.}} = \langle K_{11} \rangle_f \quad (78)$$

$$\zeta_{\text{eff.}} = \mu_s \langle \zeta \rangle_s - \frac{2}{3}\mu_s(1 - \phi) \quad (79)$$

$$\eta_{\text{eff.}}^{lm} = 2\mu_s \langle e_y(\bar{\chi}^{lm}) \rangle_s \quad (80)$$

$\eta_{\text{eff.}}$ is a fourth order tensor. It is a supplementary viscosity, capturing the grain scale anisotropy of the cell domain. With these symmetry reductions, there are now only four material parameters to be solved for: $\langle K_{11} \rangle_f$, $\langle \zeta \rangle_s$, $\langle e_{y,11}(\bar{\chi}^{11}) \rangle_s$, and $\langle e_{y,12}(\bar{\chi}^{12}) \rangle_s$ corresponding to the macroscopic permeability, bulk viscosity and two effective components of an anisotropic viscosity. Additional details of the symmetry simplifications may be found in Appendix E.

If we now define $\mathbf{V}^s \equiv \mathbf{v}^{s(0)}$, $\mathbf{V}^f \equiv \langle \mathbf{v}^{f(0)} \rangle_f / \phi$, and $P \equiv p^{f(0)}$, and drop the x subscripts from the derivatives, the above equations become (36a – 36c) presented in Section 2.4.

4. Discussion

We have successfully used homogenization to derive three macroscopic models for conservation of momentum in partially molten systems. We now consider these models further, compare them with previous models derived using multiphase flow methods and discuss some caveats and future directions.

4.1. Remarks on Homogenization Models

The differences amongst the three models of Section 2.4 arise from the assumptions on two dimensionless numbers, \mathcal{V} and \mathcal{M} , and the microstructure. All three rely on the additional assumptions that $Q_\ell^f = O(\epsilon)$ and $\mathcal{P} = O(1)$. It is helpful to write the three models as a unified set of equations:

$$0 = \bar{\rho}\mathbf{g} - \nabla P + \nabla \left[\left(\zeta_{\text{eff.}} - \frac{2}{3}\mu_s(1 - \phi) \right) \nabla \cdot \mathbf{V}^s \right] \quad (81a)$$

$$+ \nabla \cdot [2(1 - \phi)\mu_s e(\mathbf{V}^s) + 2\eta_{\text{eff.}}^{lm} e_{lm}(\mathbf{V}^s)] \quad (81b)$$

$$\phi(\mathbf{V}^f - \mathcal{V}^{-1}\mathbf{V}^s) = -\frac{k_{\text{eff.}}}{\mu_f} (\nabla P + \mathbf{g}^f)$$

$$\nabla \cdot [\phi\mathbf{V}^f + \mathcal{V}^{-1}(1 - \phi)\mathbf{V}^s] = 0 \quad (81c)$$

274 As \mathcal{V} varies from $O(\epsilon^0)$ to $O(\epsilon^{-1})$, we transition between Biphasic-I and Biphasic-II.
 275 Letting the pore network disconnect, $k_{\text{eff.}} \rightarrow 0$. Consequently, $\mathbf{V}^f \rightarrow \mathcal{V}^{-1}\mathbf{V}^s$ in (81b).
 276 This recovers macroscopic incompressibility in (81c), $\nabla \cdot \mathbf{V}^s = 0$. The divergence terms
 277 also drop from the matrix force balance equation. Making rigorous mathematical sense
 278 of the transition between the connected and disconnected pore network is an important
 279 open problem. It is also interesting that the scalings do not fully describe the macroscopic
 280 equations; the grain scale structure can play a role.

281 We return to our motivating problem, partially molten rock in the asthenosphere. As
 282 we saw in Section 2.3, for a given ϵ , the parameters \mathcal{V} and \mathcal{M} include a range where
 283 a macroscopic description is possible. We lose our ability to homogenize when either
 284 $\mathcal{M}\mathcal{V} \gg \epsilon^2$ or $\mathcal{M}\mathcal{V} \ll \epsilon^2$. There may be interesting transitions here. That the two
 285 parameters must be related by $\mathcal{M}\mathcal{V} = O(\epsilon^2)$ would seem a serious constraint on this
 286 approach and its applicability; however, this has another interpretation.

The condition on \mathcal{MV} stipulates that the length scales, viscosities, and velocities, be related by

$$L = \ell \sqrt{\frac{\mu_s V^s}{\mu_f V^f}} \quad (82)$$

This also assumes $\mathcal{P} = O(1)$. This can be reinterpreted as the macroscopic length scale on which, given the viscosities and characteristic velocities of a partially molten mix we should *expect* to observe a biphasic, viscously deformable, porous media. Based on our estimates on the viscosities, velocities, and grain scale in Table 3,

$$L \approx 10^{-1} - 10^5 \text{ km} \quad (83)$$

Length (82) is similar, but not identical to the compaction length of *McKenzie* [1984],

$$\delta_{\text{M84}} = \sqrt{\frac{\kappa(1-\phi)(\zeta_s + \frac{4}{3}\mu_s)}{\mu_f}} \quad (84)$$

287 The general scaling is similar as $\kappa \propto \ell^2$ therefore the leading scaling is $\ell\sqrt{\mu_s/\mu_f}$. Nev-
 288 ertheless δ_{M84} is porosity dependent through both permeability, κ and the viscosities, ζ_s
 289 and μ_s , making it dynamically and spatially varying. To understand the variation in
 290 compaction length, it is critical to calculate both permeabilities and viscosities that are
 291 consistent with the underlying microstructure. Homogenization provides this computa-
 292 tional machinery through the cell problems. The companion paper calculates consistent
 293 constitutive relations for several simple pore microstructures and suggests that in the limit
 294 $\phi \rightarrow 0$, $\delta_{\text{M84}} \rightarrow 0$ which has important implications for the transition to melt-free regions.
 295 However, L is not a substitute for δ_{M84} ; such a subsidiary length scale may also appear.

Under the assumption that $\mathcal{V} = O(1)$, (82) also bears resemblance to the compaction length of *Ricard et al.* [2001],

$$\delta_{\text{BRS01}} = \sqrt{\frac{\kappa_0 \mu_s}{\mu_f}} \quad (85)$$

296 κ_0 is a geometric prefactor in a power law scalar permeability relationship $\kappa = \kappa_0\phi^n$ and
 297 $\kappa_0 \propto \ell^2$.

4.2. Comparison with Existing Models

298 There are several interesting and important differences between our results and previous
 299 models derived using multiphase flow methods. Most fundamental is that we begin with
 300 a grain scale model, assume certain scalings, and formally derive a macroscopic model.
 301 The anticipated constitutive laws also emerge from these assumptions.

In the limit of large viscosity variations, the conservation of momentum equations in previous models can be closely identified with the Biphasic-I model, where $\mathcal{V} = O(1)$ and $\mathcal{M} = O(\epsilon^2)$, given by equations (36a – 36c), providing some validation. Compare with *McKenzie* [1984],

$$\partial_t (\rho_f \phi) + \nabla \cdot (\rho_f \phi \mathbf{V}^f) = \text{mass transfer} \quad (86a)$$

$$\partial_t [\rho_s(1 - \phi)] + \nabla \cdot [\rho_s(1 - \phi) \mathbf{V}^s] = -\text{mass transfer} \quad (86b)$$

$$\phi(\mathbf{V}^f - \mathbf{V}^s) = -\frac{\kappa}{\mu_f}(\nabla P - \mathbf{g}^f) \quad (86c)$$

$$0 = \bar{\rho} \mathbf{g} - \nabla P + \nabla \cdot [2(1 - \phi)\mu_s e(\mathbf{V}^s)] + \nabla \cdot \left[(1 - \phi) \left(\zeta_s - \frac{2}{3}\mu_s \right) \nabla \cdot \mathbf{V}^s \right] \quad (86d)$$

302 κ , μ_s , and ζ_s are the permeability, shear viscosity, and bulk viscosity, which have unspeci-
 303 fied dependencies on porosity. We have reused the symbols \mathbf{V}^f , \mathbf{V}^s , and P , to denote the
 304 macroscopic fluid and solid velocities, and pressure.

305 In the absence of melting and freezing, there is good agreement between the two models
 306 if we make the identifications $\zeta_{\text{eff}} \equiv \zeta_s$ and $k_{\text{eff}} \equiv \kappa$. The main difference is the appearance
 307 η_{eff} term in (36a), reflecting our consideration of a microstructure. We emphasize that

308 this macroscopic anisotropy is geometric in origin; the grain scale model was isotropic in
 309 each phase.

Now we compare with *Bercovici and Ricard* [2003], in the “geologically relevant limit” described by the authors in their Section 3.1. With a bit of algebra, and using our notation, this can be written as:

$$\partial_t \phi + \nabla \cdot (\phi \mathbf{V}^f) = 0 \quad (87a)$$

$$\partial_t(1 - \phi) + \nabla \cdot [(1 - \phi) \mathbf{V}^s] = 0 \quad (87b)$$

$$\phi(\mathbf{V}^f - \mathbf{V}^s) = -\frac{\kappa}{\mu_f}(\nabla P - \mathbf{g}^f) \quad (87c)$$

$$0 = \bar{\rho} \mathbf{g} - \nabla P + \nabla \cdot [2(1 - \phi)\mu_s e(\mathbf{V}^s)] + \nabla \cdot \left[(1 - \phi) \left(\mu_s \frac{C_0}{\phi} - \frac{2}{3} \mu_s \right) \nabla \cdot \mathbf{V}^s \right] \quad (87d)$$

+ ∇ (surface energy and damage)

310 In this model, C_0 is a dimensionless, $O(1)$ constant. The surface energy and damage
 311 terms, which we have not reproduced, capture surface physics and grain deformation. In
 312 the absence of these physics, there is again good agreement between Biphasic-I and this
 313 model if we make the identifications $\zeta_{\text{eff.}} \equiv \mu_s C_0 \phi^{-1}$ and $k_{\text{eff.}} \equiv \kappa$. As with the McKenzie
 314 model, the principal difference comes from the $\eta_{\text{eff.}}$ term. *Bercovici and Ricard* [2003]
 315 noted that if one eliminates mass transfer in (86a – 86d) and surface physics from (87a –
 316 87d), the two models are identical subject to the identification $\zeta_s \equiv \mu_s C_0 \phi^{-1}$.

317 The microscale model we homogenized, assuming only fluid dynamical coupling between
 318 the phases, was sufficient to generate macroscopic equations consistent with previous
 319 models in the absence of grain-scale surface energies. An important open problem is to
 320 find a grain scale model amenable to homogenization, that includes grain scale diffusion.
 321 One might then see a consistent macroscopic manifestation of these physics, which could

322 be compared to models that have already attempted to included them [e.g., *Ricard and*
 323 *Bercovici, 2003; Hier-Majumder et al., 2006*].

324 As mentioned previously, an advantage of the homogenization derivation over the mul-
 325 tiphase flow derivation is that there is not the same need for closures. In other models,
 326 one may posit and then seeks closures for permeability, bulk viscosity, shear viscosity, and
 327 interphase force. These parameters might be constrained by other information; however,
 328 this will not yield an inherently self-consistent model. One particularly difficult closure is
 329 the interphase force, the force that one phase exerts on the other. The interphase force,
 330 which is a macroscopic re-expression of the melt-matrix boundary conditions, is poorly
 331 constrained and non-unique. Indeed, the model in *Bercovici et al. [2001a]*, using one inter-
 332 phase force could not replicate the model of *McKenzie [1984]*. An equally valid interphase
 333 force led to (87a – 87d). As noted, taking out the additional physics, this agrees with
 334 (86a–86d). Though this a desirable result, the non-uniqueness of the terms remains an
 335 issue.

4.3. Some Caveats

336 Homogenization provides a more rigorous method for derivation of macroscopic equa-
 337 tions as well as a clear mechanism for computing critical closures. Nevertheless, it is
 338 not foolproof and includes its own set of assumptions whose consequences need to be
 339 understood.

For example, if the cell domains of Section 2.1 are independent of \mathbf{x} , then the porosity
 is constant:

$$\phi = \int_{Y_f} 1 d\mathbf{y}.$$

340 But a perfectly periodic microstructure is unrealistic. Furthermore, once motion begins,
341 the interface moves, likely breaking the periodic structure. If the domains do have \mathbf{x}
342 dependence, $Y_f = Y_f(\mathbf{x})$, then we can have $\phi = \phi(\mathbf{x})$. This introduces technical difficulties
343 in (53a), as additional terms for gradients with respect to the domain should now appear.
344 See Appendix F for details.

345 A similar omission has been made in the poro-elastic literature [see *Lee and Mei*,
346 1997a, b, c; *Lee*, 2004, for a discussion]. As the elastic matrix deforms, the interface
347 moves, changing the cell geometry. Earlier work *Auriault* [1991a]; *Hornung* [1997]; *Mei*
348 *and Auriault* [1989] implicitly assumed that this deformation was small compared to the
349 grain scale and could be ignored. This issue also bedevils the sintering and metallurgy
350 papers *Auriault et al.* [1992] and *Geindreau and Auriault* [1999]. In high temperature, tex-
351 turally equilibrated systems as might be expected in the asthenosphere, grain-boundary
352 surface forces may help to maintain the geometry of the micro-structure even during
353 large deformations. However, a consistent homogenization would need to include these
354 additional microscale processes.

355 Despite this obstacle, our equations are still of utility in several ways. The first is
356 that they are a macroscopic description of a constant porosity piece of material. Such a
357 description has not been rigorously derived before for partially molten rock. It also acts as
358 a tool for verifying the multiphase flow models. Taking ϕ to be instantaneously uniform,
359 such a model should reduce to our equations. Under simplifications, the other models,
360 such as *McKenzie* [1984]; *Bercovici and Ricard* [2003], are in agreement, up to the η_{eff} .
361 expression.

Another interpretation is that our models are valid when porosity varies sufficiently slowly. Under such an assumption, the omitted terms would be higher order in ϵ and could be justifiably dropped. There is a certain appeal to this; it would not make sense to discuss the homogenization of a material in which there were tremendous contrasts in the porosity over short length scales. Moreover, the typical porosity is $O(1\%)$, so that if the porosity parameter were also scaled, these terms may indeed be small. Such assumptions of slowly varying porosity underly all of the multiphase flow derivations (and general continuum mechanics approaches).

Our final interpretation is that the equations are part of a hierarchical model for partial melts. If we ignore melting and assume constant densities, conservation of mass can be expressed as

$$\partial_t (1 - \phi) + \nabla \cdot [(1 - \phi)\mathbf{V}^s] = 0 \quad (88)$$

We might then assume that the grain matrix may be approximated by some periodic structure at each instant. This is consistent with observations. Although the matrix deforms viscously, it retains a granular structure. Our equations are then treated as the macroscopic force balances to determine \mathbf{V}^s , and the system evolves accordingly.

Another issue with the homogenization approach is that though it illuminates how the effective viscosities and the permeability arise through the cell problems, calculating the relationship between ζ_{eff} , η_{eff} , and k_{eff} and the microstructure (e.g. porosity), requires numerically solving the cell problems. The companion paper, *Simpson et al.* [2008b], explores this, calculating effective constitutive relationships for several idealized pore geometries.

4.4. Open Problems

379 There are several ways this work might be extended. A natural continuation is to
 380 model the partial melt as a random medium. This might more realistically model the
 381 pore structure of rocks. The equations for upscaling could also be augmented by giving
 382 the matrix a nonlinear rheology, as in *Auriault et al.* [1992]; *Geindreau and Auriault* [1999].
 383 This may be particularly important for magma migration; a nonlinear matrix rheology
 384 was needed to computationally model physical experiments for shear bands in *Katz et al.*
 385 [2006] and in general, non-linear power-law rheologies are expected in the dislocation creep
 386 regime [e.g., *Hirth and Kohlstedt*, 1995b].

387 Important mechanisms absent from these equations are surface physics which. In a fluid
 388 dynamical description, these might take the form as surface tension and diffusional terms.
 389 Such terms were posited in the models of *Ricard et al.* [2001]; *Hier-Majumder et al.* [2006];
 390 *Bercovici and Ricard* [2005, 2003]; *Bercovici et al.* [2001b, a], but it remains to be shown
 391 how such terms in the macroscopic equations might arise consistently from microscopic
 392 physics that includes grain-scale diffusion and/or mass transfer.

393 The most serious question remains how to a properly study a medium with macroscopic
 394 and time dependent variations in the structure. This would have implications for the
 395 many physical phenomena that also have *evolving microstructures*. Recent work in *Peter*
 396 [2007a, b, 2009] on reaction-diffusion systems in porous media may be applicable.

Appendix A: Details of the Expansions

The multiple scale expansions of (8) are applied to \tilde{p}^s , \tilde{p}^f , $\tilde{\mathbf{v}}^s$, $\tilde{\mathbf{v}}^f$ and substituted into the dimensionless equations (39a – 39f), along with the two scale derivatives, (41a – 41c).

Dropping tildes, both melt and matrix strain rate tensors expand as:

$$\begin{aligned} e_y(\mathbf{v}) &\mapsto \epsilon^0 [e_y(\mathbf{v}^{(0)})] + \epsilon^1 [e_x(\mathbf{v}^{(0)}) + e_y(\mathbf{v}^{(1)})] + \epsilon^2 [e_x(\mathbf{v}^{(1)}) + e_y(\mathbf{v}^{(2)})] + \dots \\ &\equiv \epsilon^0 e^{(0)} + \epsilon^1 e^{(1)} + \epsilon^2 e^{(2)} + \dots \end{aligned} \quad (\text{A1})$$

The stress tensors become:

$$\begin{aligned} \sigma^s &\mapsto \epsilon^{-1} [2\mu_s e^{s(0)}] + \epsilon^0 [-p^{s(0)} I + 2\mu_s e^{s(1)}] + \epsilon^1 [-p^{s(1)} I + 2\mu_s e^{s(2)}] + \dots \\ &\equiv \epsilon^{-1} \sigma^{s(-1)} + \epsilon^0 \sigma^{s(0)} + \epsilon^1 \sigma^{s(1)} + \dots \end{aligned} \quad (\text{A2a})$$

$$\begin{aligned} \sigma^f &\mapsto \epsilon^0 [-p^{f(0)} I] + \epsilon^1 [-p^{f(1)} I + 2\mu_f e^{f(0)}] + \epsilon^2 [-p^{f(2)} I + 2\mu_f e^{f(1)}] + \dots \\ &\equiv \sigma^{f(0)} + \epsilon^1 \sigma^{f(1)} + \epsilon^2 \sigma^{f(2)} + \dots \end{aligned} \quad (\text{A2b})$$

Matching powers of ϵ in equations (A2a) and (A2b) in (39a) and (39b)

$$\begin{aligned} \epsilon^{-1} \nabla_y \cdot \sigma^{s(-1)} + \epsilon^0 (\nabla_x \cdot \sigma^{s(-1)} + \nabla_y \cdot \sigma^{s(0)}) + \epsilon^1 (\nabla_x \cdot \sigma^{s(0)} + \nabla_y \cdot \sigma^{s(1)} + \mathbf{g}^s) \\ + \dots = 0 \end{aligned} \quad (\text{A3a})$$

$$\begin{aligned} \epsilon^0 \nabla_y \cdot \sigma^{f(0)} + \epsilon^1 (\nabla_x \cdot \sigma^{f(0)} + \nabla_y \cdot \sigma^{f(1)} + \mathbf{g}^f) + \epsilon^2 (\nabla_x \cdot \sigma^{f(1)} + \nabla_y \cdot \sigma^{f(2)}) \\ + \dots = 0 \end{aligned} \quad (\text{A3b})$$

Analogously, we substitute the expansions into the incompressibility equations (39c–39d), to get

$$\begin{aligned} \epsilon^0 \nabla_y \cdot \mathbf{v}^{f(0)} + \epsilon^1 (\nabla_x \cdot \mathbf{v}^{f(0)} + \nabla_y \cdot \mathbf{v}^{f(1)}) + \dots = 0 \\ \epsilon^0 \nabla_y \cdot \mathbf{v}^{s(0)} + \epsilon^1 (\nabla_x \cdot \mathbf{v}^{s(0)} + \nabla_y \cdot \mathbf{v}^{s(1)}) + \dots = 0 \end{aligned} \quad (\text{A4})$$

³⁹⁷ The leading order equations of (A4), $\nabla_y \cdot \mathbf{v}^{f(0)} = 0$ and $\nabla_y \cdot \mathbf{v}^{s(0)} = 0$, reflect that at the
³⁹⁸ grain scale, both phases are incompressible.

Making the same power series expansions in the boundary conditions, continuity of normal stress, (39e), is

$$\epsilon^{-1} \sigma^{s(-1)} \cdot \mathbf{n} + \epsilon^0 (\sigma^{s(0)} - \sigma^{f(0)}) \cdot \mathbf{n} + \dots = 0. \quad (\text{A5})$$

When $\mathcal{V} = O(1)$, the velocity boundary condition within the cell is

$$\epsilon^0 (\mathbf{v}^{s(0)} - \mathbf{v}^{f(0)}) + \epsilon^1 (\mathbf{v}^{s(1)} - \mathbf{v}^{f(1)}) + \dots = 0 \quad \text{on } \gamma. \quad (\text{A6})$$

In this case, the velocities are matched at all orders of ϵ . If instead $\mathcal{V} = O(\epsilon^{-1})$, then

$$\begin{aligned} \epsilon^{-1} \mathbf{v}^{f(0)} + \epsilon^0 (\mathbf{v}^{f(1)} - \mathbf{v}^{s(0)}) \\ + \epsilon^1 (\mathbf{v}^{f(2)} - \mathbf{v}^{s(1)}) + \dots = 0 \quad \text{on } \gamma. \end{aligned} \tag{A7}$$

399 In contrast to the $\mathcal{V} = O(1)$ case, the leading order fluid velocity is independent of the
400 solid, and there is cross coupling across orders.

Appendix B: Cell Problems in the Matrix

401 In general, there are two classes of cell problems associated with the matrix phase, and
402 a total of seven cell problems. Domain symmetry can reduce the number of unique cell
403 problems.

B1. Cell Problem for Dilation Stress on Solid

This addresses the term $\nabla_x \cdot \mathbf{v}^{s(0)}$ in (50b). This is a less common Stokes problem, with a prescribed function in the divergence equation. They are briefly discussed in *Temam* [2001]. Let $\bar{\xi}$, $\bar{\zeta}$ be \mathbf{y} periodic functions solving

$$\nabla_y \cdot (-\bar{\zeta}I + 2e_y(\bar{\xi})) = 0 \quad \text{in } Y_s \tag{B1a}$$

$$\nabla_y \cdot \bar{\xi} = 1 \quad \text{in } Y_s \tag{B1b}$$

$$(-\bar{\zeta}I + 2e_y(\bar{\xi})) \cdot \mathbf{n} = 0 \quad \text{on } \gamma \tag{B1c}$$

404 The solution measures the response of a unit cell of the matrix to the divergence condition
405 (B1b).

B2. Cell Problem for Surface Stresses on Solid

This problem tackles the boundary stress in (50c). Let $\bar{\chi}^{lm}$, π^{lm} be \mathbf{y} periodic functions solving

$$\nabla_{\mathbf{y}} \cdot (-\pi^{lm} I + 2e_{\mathbf{y}}(\bar{\chi}^{lm})) = 0 \quad \text{in } Y_s \quad (\text{B2a})$$

$$\nabla_{\mathbf{y}} \cdot \bar{\chi}^{lm} = 0 \quad \text{in } Y_s \quad (\text{B2b})$$

$$(-\pi^{lm} \delta_{ij} + 2e_{\mathbf{y},ij}(\bar{\chi}^{lm})) n_j = -\frac{1}{2} (\delta_{il} \delta_{jm} + \delta_{im} \delta_{jl}) n_j \quad \text{on } \gamma \quad (\text{B2c})$$

406 $(\bar{\chi}^{lm}, \pi^{lm})$ measure the response of a unit cell of the matrix to a given unit surface stress,
 407 depending on indices (l, m) . Observe that because the tensor on the right hand side of
 408 (B2c), operating on \mathbf{n} , is symmetric, the solution to problem (l, m) is the same as the
 409 solution for problem (m, l) . For general domains, there are thus six unique cell problems
 410 associated with surface stress forcing.

Appendix C: Additional Scaling Regimes

411 In addition to the Biphasic-I regime which we derived in Section 3.5, we presented two
 412 other cases in Section 2.4. These are Biphasic-II, where $\mathcal{V} = O(\epsilon^{-1})$ and $\mathcal{M} = O(\epsilon^3)$, and
 413 Monophasic, where assumes $\mathcal{V} = O(1)$ and $\mathcal{M} = O(\epsilon^2)$ and additionally assumes the melt
 414 network is disconnected. Their derivation is given in the next two sections.

C1. Biphasic-II: Unequal Velocities at the Interface

In this case $\mathcal{V} = O(\epsilon^{-1})$ and $\mathcal{M} = O(\epsilon^3)$. Following the scheme of Section 3.5, the macroscopic equations are

$$\langle \mathbf{v}^{f(0)} \rangle_f = -\frac{\langle K \rangle_f}{\mu_f} (\nabla_x p^{f(0)} - \mathbf{g}^f) \quad (\text{C1})$$

$$\nabla_x \cdot \langle \mathbf{v}^{f(0)} \rangle_f = 0. \quad (\text{C2})$$

415 Multiplying (C1) by V^f and (C2) by V^f/L restores the dimensions of these equations.

C2. Monophasic: Magma Bubbles

416 As in Biphasic-I, we take $\mathcal{V} = O(1)$ and $\mathcal{M} = O(\epsilon^2)$. However, we now assume that the
 417 fluid is not topologically connected. The equations are the same at all orders of ϵ as those
 418 appearing in Section 3.5.

Under this assumption on the microscopic geometry, the permeability cell problems, (64a–64c), can be shown to have trivial solutions. $\mathbf{k}^i = 0$ for $i = 1, 2, 3$, so $\langle k \rangle_f = 0$. Because the melt is trapped it must migrate with the matrix,

$$\mathbf{v}^{f(0)}(\mathbf{x}, \mathbf{y}) = \mathbf{v}^{s(0)}(\mathbf{x}) \quad (\text{C3})$$

Combining (C3) with (74), recovers the incompressibility of the matrix,

$$\nabla_x \cdot \mathbf{v}^{s(0)} = 0 \quad (\text{C4})$$

Dropping the divergence terms from (59) completes the system:

$$\begin{aligned} 0 = & \bar{\rho} \mathbf{g} - \nabla_x p^{f(0)} - \nabla_x [2\mu_s e_{x,lm}(\mathbf{v}^{s(0)}) \langle \pi^{lm} \rangle_s] \\ & + 2\mu_s \nabla_x \cdot [(1 - \phi) e_x(\mathbf{v}^{s(0)}) + 2e_{x,lm}(\mathbf{v}^{s(0)}) \langle e_y(\bar{\chi}^{lm}) \rangle_s] \end{aligned} \quad (\text{C5})$$

419 This is a homogenized incompressible Stokes system for a hybrid material with isolated
 420 very low viscosity inclusions.

Appendix D: Non-Homogenizable Regimes

When either $Q_\ell^f \gg \epsilon$ or $Q_\ell^f \ll \epsilon$, the system is non-homogenizable. By this we mean that it is not possible to upscale equations that faithfully preserve our physical assumptions. For instance, if $Q_\ell^f = O(1)$ the pressure gradient balances the viscous forces in the fluid and there is no scale separation. Working out the expansions, the leading order velocity

and pressure in the fluid solve:

$$\nabla_y \cdot [-\tilde{p}^{f(0)} + 2\tilde{\mu}_f e_y(\tilde{\mathbf{v}}^{f(0)})] = 0 \quad \text{in } Y_f \quad (\text{D1})$$

$$\nabla_y \cdot \tilde{\mathbf{v}}^{f(0)} = 0, \quad \text{in } Y_f \quad (\text{D2})$$

$$\tilde{\mathbf{v}}^{f(0)} = 0, \quad \text{on } \gamma \quad (\text{D3})$$

The solution is $\tilde{\mathbf{v}}^{f(0)} = 0$. Therefore,

$$\begin{aligned} \mathbf{v}^{f,\epsilon} &= V^f \tilde{\mathbf{v}}^{f,\epsilon} \\ &= V^f (\tilde{\mathbf{v}}^{f(0)} + \epsilon \tilde{\mathbf{v}}^{f(1)} + \dots) \\ &= \epsilon V^f (\mathbf{v}^{f(1)} + \dots) \end{aligned} \quad (\text{D4})$$

421 This implies that $|\mathbf{v}^{f,\epsilon}| = O(\epsilon V^f)$, contradicting our physical assumption that $|\mathbf{v}^{f,\epsilon}| =$
 422 $O(V^f)$. While this is mathematically reasonable, the model is unable to produce macro-
 423 scopic fluid velocities of order V^f . Other upscaling techniques may succeed here, but
 424 homogenization will not.

Suppose instead $Q_\ell^f = O(\epsilon^2)$ or smaller. The fluid equations are then:

$$O(\epsilon^0): \quad -\nabla_y \tilde{p}^{f(0)} = 0 \quad \text{in } Y_f \quad (\text{D5})$$

$$O(\epsilon^1): \quad -\nabla_y \tilde{p}^{f(1)} - \nabla_x \tilde{p}^{f(0)} + \tilde{\mathbf{g}}^f = 0 \quad \text{in } Y_f \quad (\text{D6})$$

The first equation implies $\tilde{p}^{f(0)} = \tilde{p}^{f(0)}(\mathbf{x})$. Since $\nabla_x \tilde{p}^{f(0)}$ and $\tilde{\mathbf{g}}^f$ are independent of \mathbf{y} , $\nabla_y \tilde{p}^{f(1)}$ must also be independent. Since it is periodic in \mathbf{y} , it is zero. But this implies

$$-\nabla_x \tilde{p}^{f(0)} + \tilde{\mathbf{g}}^f = 0 \quad (\text{D7})$$

425 *The leading order macroscopic pressure gradient plays no role in balancing the viscous*
 426 *forces in the solid.* This contradicts our assumption that there is *always* a leading order
 427 non-hydrostatic pressure gradient.

Though our assumption on the non-hydrostatic pressure gradient may seem arbitrary, there is another important reason to identify cases without such a pressure as non-homogenizable. There are problems of interest where gravity plays little role, such as *Spiegelman* [2003]; *Katz et al.* [2006]. In these cases, $\tilde{\mathbf{g}}^f$ would be absent from our equations, including (D7). Hence,

$$\begin{aligned}\nabla p^f &= \frac{P^f}{L} \nabla_x (\tilde{p}^{f(0)} + \epsilon \tilde{p}^{f(1)} + \dots) \\ &= \epsilon \frac{P^f}{L} \nabla_x (\tilde{p}^{f(1)} + \dots) \\ &= O\left(\epsilon \frac{P^f}{L}\right)\end{aligned}$$

428 This implies the macroscopic fluid pressure gradient is not $O(P^f/L)$, as hypothesized.

Appendix E: Cell Problem Symmetries

429 Let us assume our cell domain is symmetric with respect to the principal axes and
430 invariant under rigid rotations. This permits simplifications of some of the cell problems.

In the Darcy cell problem, the off-diagonal entries become zero while the diagonal entries are all equal. Thus:

$$k_{\text{eff.}} = \langle \mathbf{k}_1^1 \rangle_f \quad (\text{E1})$$

431 For the surface stress problems, when $l \neq m$, $\langle \pi^{lm} \rangle_s = 0$. Only the l, m and m, l entries
432 of the tensor $\langle e_y(\bar{\chi}^{lm}) \rangle_s$ are non-zero. For $l = m$, $\langle \pi^{ll} \rangle_s = \frac{1}{3}(1 - \phi)$ and only the diagonal
433 entries of $\langle e_y(\bar{\chi}^{ll}) \rangle_s$ are non-zero. The trace of all $\langle e_y(\bar{\chi}^{lm}) \rangle_s$ tensors is zero. More can be
434 said about $e_y(\bar{\chi}^{lm})$, but it does not benefit the present analysis. See *Simpson* [2008] or
435 *Simpson et al.* [2008b] for more details.

436 In the dilation stress problem, the off diagonal terms in $\langle e_y(\bar{\xi}) \rangle_s$ vanish, and the diagonal
437 entries are equal to $\frac{1}{3}(1 - \phi)$.

Appendix F: Spatial Variation in Cell Domain and Time Dynamics

If the cells have \mathbf{x} dependence, $Y_f = Y_f(\mathbf{x})$, then it is possible that $\phi = \phi(\mathbf{x})$. This introduces difficulties in (53a), as terms from gradients with respect to the domain now appear. Let us elaborate. For fixed $\mathbf{x} \in \Omega$, we associate a particular cell $Y = Y(\mathbf{x})$, with fluid and solid regions defined by the indicator functions \mathbb{I}_f and \mathbb{I}_s :

$$\mathbb{I}_s : \Omega \times Y \mapsto \{0, 1\} \quad (\text{F1a})$$

$$\mathbb{I}_f : \Omega \times Y \mapsto \{0, 1\} \quad (\text{F1b})$$

Then

$$Y_f(\mathbf{x}) = \{\mathbf{y} \in Y \mid \mathbb{I}_f(\mathbf{x}, \mathbf{y}) = 1\} \quad (\text{F2a})$$

$$Y_s(\mathbf{x}) = \{\mathbf{y} \in Y \mid \mathbb{I}_s(\mathbf{x}, \mathbf{y}) = 1\} \quad (\text{F2b})$$

Returning to (53a),

$$\begin{aligned} & \int_{Y_s} \nabla_x \cdot \sigma^{s(0)} d\mathbf{y} + \int_{Y_f} \nabla_x \cdot \sigma^{f(0)} d\mathbf{y} \\ &= \int_Y \nabla_x \cdot \sigma^{s(0)} \mathbb{I}_s d\mathbf{y} + \int_Y \nabla_x \cdot \sigma^{f(0)} \mathbb{I}_f d\mathbf{y} \\ &= \nabla_x \cdot \int_{Y_s} \sigma^{s(0)} d\mathbf{y} - \int_Y \sigma^{s(0)} \cdot \nabla_x \mathbb{I}_s d\mathbf{y} \\ & \quad + \nabla_x \cdot \int_{Y_f} \sigma^{f(0)} d\mathbf{y} - \int_Y \sigma^{f(0)} \cdot \nabla_x \mathbb{I}_f d\mathbf{y} \end{aligned} \quad (\text{F3})$$

⁴³⁸ Witness the appearance of the $\nabla \mathbb{I}_s$ and $\nabla \mathbb{I}_f$ terms. *This is only an issue for (53a). The*
⁴³⁹ *other macroscopic equations remain valid when we allow cell variation.*

A second problem is manifest when we consider time dynamics.

$$\begin{aligned} \partial_t \phi &= \partial_t \int_{Y_f} 1 d\mathbf{y} = \int_{\Gamma} \mathbf{v}^f \cdot \mathbf{n} dS \\ &= - \int_{\Gamma} \mathbf{v}^s \cdot \mathbf{n} dS = - \int_{\Gamma} (\mathbf{v}^{s(0)} + \epsilon \mathbf{v}^{s(1)} + \dots) \cdot \mathbf{n} dS \end{aligned}$$

Since $\mathbf{v}^{s(0)}$ is independent of \mathbf{y} , the first term drops. Substituting (51),

$$\partial_t \phi = -\epsilon \int \nabla_y \cdot \mathbf{v}^{s(1)} d\mathbf{y} + O(\epsilon^2) = \epsilon \nabla_x \cdot \mathbf{v}^{s(0)} (1 - \phi) + O(\epsilon^2)$$

440 To leading order, the matrix can only vary by dilation and compaction.

441 **Acknowledgments.** Both this paper and *Simpson et al.* [2008b] are based on the
442 thesis of G. Simpson, *Simpson* [2008], completed in partial fulfillment of the requirements
443 for the degree of doctor of philosophy at Columbia University.

444 The authors wish to thank D. Bercovici and R. Kohn for their helpful comments.

445 This work was funded in part by the US National Science Foundation (NSF) Collabo-
446 ration in Mathematical Geosciences (CMG), Division of Mathematical Sciences (DMS),
447 Grant DMS-05-30853, the NSF Integrative Graduate Education and Research Trainee-
448 ship (IGERT) Grant DGE-02-21041, NSF Grants DMS-04-12305 and DMS-07-07850.

References

- 449 Auriault, J., Nonsaturated deformable porous media: Quasistatics, *Transport in Porous*
450 *Media*, 2(1), 45–64, 1987.
- 451 Auriault, J., Heterogeneous medium. Is an equivalent macroscopic description possible?,
452 *International Journal of Engineering Science*, 29(7), 785–795, 1991a.
- 453 Auriault, J., Poroelastic media, in *Homogenization and Porous Media*, edited by U. Hor-
454 nung, pp. 163–182, Springer, 1991b.
- 455 Auriault, J., and C. Boutin, Deformable porous media with double porosity. Quasi-static.
456 I: Coupling effects, *Transport in Porous Media*, 7(1), 63–82, 1992.
- 457 Auriault, J., and P. Royer, Seismic waves in fractured porous media, *Geophysics*, 67, 259,
458 2002.
- 459 Auriault, J., D. Bouvard, C. Dellis, and M. Lafer, Modelling of Hot Compaction of Metal
460 Powder by Homogenization, *Mechanics of Materials(The Netherlands)*, 13(3), 247–255,

- 461 1992.
- 462 Bensoussan, A., J. Lions, and G. Papanicolaou, *Asymptotic Analysis for Periodic Structures*, *Studies in Mathematics and its Applications*, vol. 5, Elsevier, 1978.
- 463
- 464 Bercovici, D., and Y. Ricard, Energetics of a two-phase model of lithospheric damage, shear localization and plate-boundary formation, *Geophysical Journal International*,
- 465
- 466 152(3), 581–596, 2003.
- 467 Bercovici, D., and Y. Ricard, Tectonic plate generation and two-phase damage: Void growth versus grain size reduction, *Journal of Geophysical Research*, 110(B3), 2005.
- 468
- 469 Bercovici, D., Y. Ricard, and G. Schubert, A two-phase model for compaction and damage, 1: General theory, *Journal of Geophysical Research*, 106(B5), 8887–8906, 2001a.
- 470
- 471 Bercovici, D., Y. Ricard, and G. Schubert, A Two-Phase Model for Compaction and Damage, 3: Applications to Shear Localization and Plate Boundary Formation, *Journal*
- 472
- 473 *of Geophysical Research*, 106, 8925–8939, 2001b.
- 474 Brennen, C., *Fundamentals of Multiphase Flow*, Cambridge University Press, 2005.
- 475 Chechkin, G., A. Piatnitski, and A. Shamaev, *Homogenization: Methods and Applications*, Translations of Mathematical Monographs, American Mathematical Society, 2007.
- 476
- 477 Cioranescu, D., and P. Donato, *An Introduction to Homogenization*, Oxford University Press, 1999.
- 478
- 479 Drew, D., Averaged field equations for two-phase media, *Stud. Appl. Math*, 50(2), 133–
- 480 166, 1971.
- 481 Drew, D., Mathematical-modeling of 2-phase flow, *Ann. Rev. Fluid Mech*, 15, 261–291, 1983.
- 482
- 483 Drew, D., and S. Passman, *Theory of multicomponent fluids*, Springer New York, 1999.

- 484 Drew, D., and L. Segel, Averaged equations for two-phase flows, *Stud. Appl. Math*, 50(3),
485 205–231, 1971.
- 486 Fowler, A., A mathematical model of magma transport in the asthenosphere, *Geophysical*
487 *& Astrophysical Fluid Dynamics*, 33(1), 63–96, 1985.
- 488 Fowler, A., Generation and Creep of Magma in the Earth, *SIAM Journal on Applied*
489 *Mathematics*, 49, 231, 1989.
- 490 Geindreau, C., and J. Auriault, Investigation of the viscoplastic behaviour of alloys in the
491 semi-solid state by homogenization, *Mechanics of Materials*, 31(8), 535–551, 1999.
- 492 Hier-Majumder, S., Y. Ricard, and D. Bercovici, Role of grain boundaries in magma
493 migration and storage, *Earth and Planetary Science Letters*, 248(3-4), 735–749, 2006.
- 494 Hirth, G., and D. Kohlstedt, Experimental constraints on the dynamics of the partially
495 molten upper mantle: Deformation in the diffusion creep regime, *Journal of Geophysical*
496 *Research*, 100(B2), 1981–2001, 1995a.
- 497 Hirth, G., and D. Kohlstedt, Experimental constraints on the dynamics of the partially
498 molten upper mantle 2: Deformation in the dislocation creep regime, *Journal of Geo-*
499 *physical Research*, 100(B2), 15,441–15,449, 1995b.
- 500 Hornung, U., *Homogenization and Porous Media*, Springer, 1997.
- 501 Katz, R., M. Spiegelman, and B. Holtzman, The dynamics of melt and shear localization
502 in partially molten aggregates., *Nature*, 442(7103), 676–9, 2006.
- 503 Katz, R., M. Knepley, B. Smith, M. Spiegelman, and E. Coon, Numerical simulation of
504 geodynamic processes with the Portable Extensible Toolkit for Scientific Computation,
505 *Physics of the Earth and Planetary Interiors*, 163(1-4), 52–68, 2007.

- 506 Lee, C., Flow and deformation in poroelastic media with moderate load and weak iner-
507 tia, *Proceedings of the Royal Society of London. Series A, Mathematical and Physical*
508 *Sciences*, 460(2047), 2051–2087, 2004.
- 509 Lee, C., and C. Mei, Re-examination of the equations of poroelasticity, *International*
510 *journal of engineering science*, 35(4), 329–352, 1997a.
- 511 Lee, C., and C. Mei, Thermal consolidation in porous media by homogenization theory—
512 I. Derivation of macroscale equations, *Advances in Water Resources*, 20(2-3), 127–144,
513 1997b.
- 514 Lee, C., and C. Mei, Thermal consolidation in porous media by homogenization theory—
515 II. Calculation of effective coefficients, *Advances in Water Resources*, 20(2-3), 145–156,
516 1997c.
- 517 McKenzie, D., The generation and compaction of partially molten rock, *Journal of Petrol-*
518 *ogy*, 25(3), 713–765, 1984.
- 519 Mei, C., and J. Auriault, Mechanics of Heterogeneous Porous Media With Several Spatial
520 Scales, *Proceedings of the Royal Society of London. Series A, Mathematical and Physical*
521 *Sciences*, 426(1871), 391–423, 1989.
- 522 Mei, C., J. Auriault, and C. Ng, Some applications of the homogenization theory, *Advances*
523 *in applied mechanics*, 32, 277–348, 1996.
- 524 Pavliotis, G., and A. Stuart, *Multiscale Methods: Averaging and Homogenization*,
525 Springer, 2008.
- 526 Peter, M., Homogenisation of a chemical degradation mechanism inducing an evolving
527 microstructure, *Comptes rendus-Mécanique*, 335(11), 679–684, 2007a.

- 528 Peter, M., Homogenisation in domains with evolving microstructure, *Comptes rendus-*
529 *Mécanique*, *335*(7), 357–362, 2007b.
- 530 Peter, M., Coupled reaction–diffusion processes inducing an evolution of the microstruc-
531 ture: Analysis and homogenization, *Nonlinear Analysis*, *70*, 806–821, 2009.
- 532 Ricard, Y., Physics of mantle convection, in *Treatise on Geophysics*, vol. 7, edited by
533 G. Schubert, Elsevier, 2007.
- 534 Ricard, Y., and D. Bercovici, Two-phase damage theory and crustal rock failure: the
535 theoretical ‘void’ limit, and the prediction of experimental data, *Geophysical Journal*
536 *International*, *155*(3), 1057–1064, 2003.
- 537 Ricard, Y., D. Bercovici, and G. Schubert, A two-phase model of compaction and damage,
538 2: Applications to compaction, deformation, and the role of interfacial surface tension,
539 *Journal of Geophysical Research*, *106*, 8907–8924, 2001.
- 540 Sanchez-Palencia, E., *Non-homogeneous media and vibration theory*, Lecture Notes in
541 Physics, 127, 1980.
- 542 Schmeling, H., Partial melting and melt segregation in a convecting mantle, in *Physics*
543 *and Chemistry of Partially Molten Rocks*, edited by N. Bagdassarov, D. Laporte, and
544 A. Thompson, pp. 141–178, Kluwer Academic, 2000.
- 545 Scott, D., and D. Stevenson, Magma solitons, *Geophysical Research Letters*, *11*(11), 1161–
546 1161, 1984.
- 547 Scott, D., and D. Stevenson, Magma ascent by porous flow, *Journal of Geophysical Re-*
548 *search*, *91*, 9283–9296, 1986.
- 549 Simpson, G., The mathematics of magma migration, Ph.D. thesis, Columbia University,
550 2008.

- 551 Simpson, G., M. Spiegelman, and M. Weinstein, A multiscale model of partial melts 1:
552 Effective equations, submitted to Journal of Geophysical Research, 2008a.
- 553 Simpson, G., M. Spiegelman, and M. Weinstein, A multiscale model of partial melts 2:
554 Numerical results, submitted to Journal of Geophysical Research, 2008b.
- 555 Spiegelman, M., Flow in deformable porous media. part 1: Simple analysis, *Journal of*
556 *Fluid Mechanics*, *247*, 17–38, 1993.
- 557 Spiegelman, M., Linear analysis of melt band formation by simple shear, *Geochemistry,*
558 *Geophysics, Geosystems*, *4*(9), 8615, 2003.
- 559 Spiegelman, M., R. Katz, and G. Simpson, An Introduction and Tutorial to the
560 “McKenize Equations” for magma migration, [http://www.geodynamics.org/cig/
561 workinggroups/magma/workarea/benchmark/McKenzieIntroBenchmarks.pdf](http://www.geodynamics.org/cig/workinggroups/magma/workarea/benchmark/McKenzieIntroBenchmarks.pdf), 2007.
- 562 Stevenson, D., and D. Scott, Mechanics of Fluid-Rock Systems, *Annual Review of Fluid*
563 *Mechanics*, *23*(1), 305–339, 1991.
- 564 Temam, R., *Navier-Stokes Equations: Theory and Numerical Analysis*, American Math-
565 ematical Society, 2001.
- 566 Torquato, S., *Random Heterogeneous Materials: Microstructure and Macroscopic Proper-*
567 *ties*, Springer, 2002.
- 568 Wark, D., and E. Watson, Grain-scale permeabilities of texturally equilibrated, monomin-
569 eralic rocks, *Earth and Planetary Science Letters*, *164*(3-4), 591–605, 1998.

Table 1. Notation for domains in homogenization model.

Symbol	Meaning
γ	Interface between melt and matrix within cell Y
Γ	Total macroscopic interface between melt and matrix
Ω	Total macroscopic space occupied by both melt and matrix
Ω_f	Portion of macroscopic space occupied by melt
Ω_s	Portion macroscopic space occupied by matrix
Y	The unit cell
Y_f	Portion of unit cell occupied by melt
Y_s	Portion of unit cell occupied by matrix

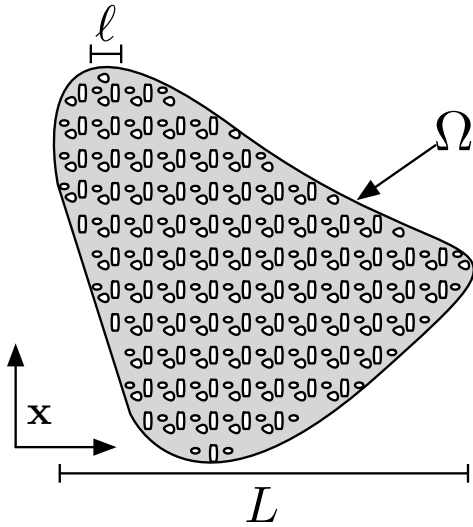


Figure 1. The macroscopic domain Ω . The matrix occupies the gray region while the melt occupies the white inclusions.

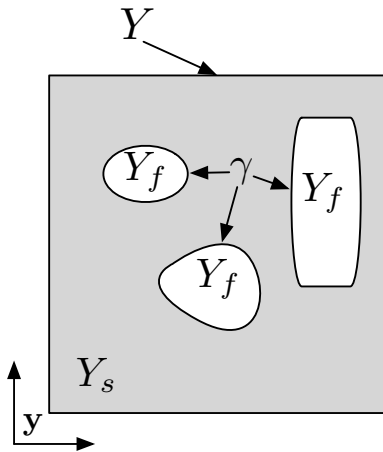


Figure 2. The cell domain, Y , divided into fluid and solid regions, Y_f and Y_s . The two phases meet on interface Γ .

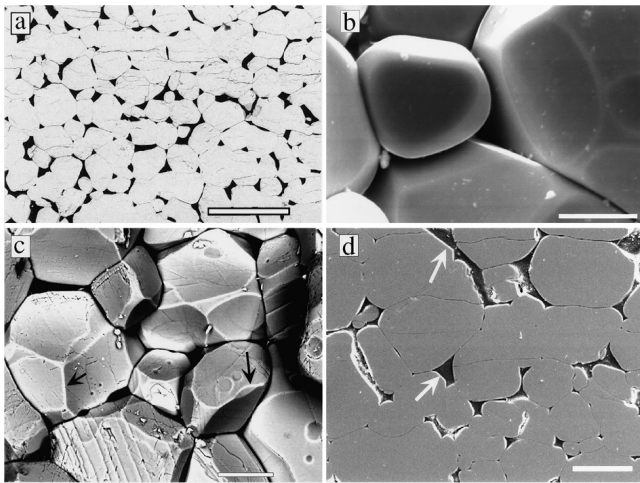


Figure 3. SEM images of synthetic quartzites and marbles from Figure 5 of *Wark and Watson* [1998]. Similar microstructures are seen in olivine basalt aggregates [e.g. *Hirth and Kohlstedt*, 1995a, b]

Table 2. Notation for fields in homogenization model.

Symbol	Meaning
$e(\mathbf{v})$	Strain rate tensor, $e(\mathbf{v}) = \frac{1}{2}(\nabla\mathbf{v} + (\nabla\mathbf{v})^T)$
ϕ	Volume fraction of melt, $\phi \equiv \int_{Y_f} d\mathbf{y}$
\mathbf{g}	$-\mathbf{g}\mathbf{z}$
\mathbf{g}^f	$\rho_f\mathbf{g}$
\mathbf{g}^s	$\rho_s\mathbf{g}$
p^f	Melt pressure
$p^{f(j)}$	Melt pressure at order j in the series expansion
p^s	Melt pressure
$p^{s(j)}$	Matrix pressure at order j in the series expansion
σ^f	Melt Stress Tensor
$\sigma^{f(j)}$	Melt Stress Tensor at order j in the series expansion
σ^s	Matrix Stress Tensor
$\sigma^{s(j)}$	Matrix Stress Tensor at order j in the series expansion
\mathbf{v}^f	Melt velocity
$\mathbf{v}^{f(j)}$	Melt velocity at order j in the series expansion
\mathbf{v}^s	Matrix Velocity
$\mathbf{v}^{s(j)}$	Matrix velocity at order j in the series expansion

Table 3. Notation and measurements for models of partial melts.

Symbol	Meaning	Value
ϕ	Volume Fraction of Melt	.01%– 10%
g	Gravity	9.8 m/s ²
ℓ	Grain Length Scale	1 –10 mm
L	Macroscopic Length Scale	1 m - 10 km
μ_f	Melt Shear Viscosity	1–10 Pa s
μ_s	Matrix Shear Viscosity	10 ¹⁵ –10 ²¹ Pa s
Re_ℓ^f	Reynolds Number of Melt	10 ⁻⁸ –10 ⁻⁵
Re_ℓ^s	Reynolds Number of Matrix	10 ⁻³⁰ –10 ⁻²²
ρ_f	Melt Density	2800 kg/m ³
ρ_s	Matrix Density	3300 kg/m ³
V^f	Characteristic Melt Velocity	1 – 10 m/yr
V^s	Characteristic Matrix Velocity	1 – 10 cm/yr

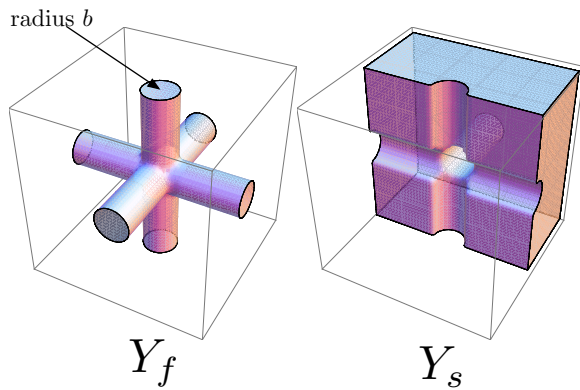


Figure 4. A cell geometry in which both the fluid region, Y_f , and the solid region, Y_s , are topologically connected.

Table 4. Dimensionless numbers for homogenization model.

Symbol	Meaning	Estimate
ϵ	Length scale ratio, $\epsilon = \ell/L$	$O(10^{-7} - 10^{-2})$
\mathcal{M}	Viscosity ratio, $\mathcal{M} = \mu_f/\mu_s$	$O(10^{-21} - 10^{-14})$
\mathcal{P}	Pressure ratio, $\mathcal{P} = P^f/P^s$	$O(\epsilon^0)$
\mathcal{Q}_ℓ^f	Ratio of viscous force to pressure gradient in melt, $\mathcal{Q}_\ell^f = (\mu_f V^f)/(P^f \ell)$	$O(\epsilon^9 - \epsilon^0)$
\mathcal{Q}_ℓ^s	Ratio of viscous force to pressure gradient in matrix, $\mathcal{Q}_\ell^s = (\mu_s V^s)/(P^s \ell)$	$O(\epsilon^{-1})$
\mathcal{Q}_L^s	Ratio of viscous force to pressure gradient in matrix, $\mathcal{Q}_L^s = (\mu_s V^s)/(P^s L)$	$O(\epsilon^0)$
\mathcal{R}_ℓ^f	Ratio of buoyancy force to pressure gradient in melt, $\mathcal{R}_\ell^f = (\rho_f g \ell)/P^f$	$O(\epsilon^1)$
\mathcal{R}_ℓ^s	Ratio of buoyancy force to pressure gradient in matrix, $\mathcal{R}_\ell^s = (\rho_s g \ell)/P^s$	$O(\epsilon^1)$
\mathcal{R}_L^s	Buoyancy force to pressure gradient ratio in matrix, $\mathcal{R}_L^s = (\rho_s g L)/P^s$	$O(\epsilon^0)$
\mathcal{V}	Velocity ratio, $\mathcal{V} = V^f/V^s$	$O(10^{-7} - 10^{-2})$

Table 5. Effective quantities derived by homogenization.

Symbol	Meaning
η_{eff}	Effective supplementary anisotropic viscosity, a fourth order tensor. $\eta_{\text{eff}}^{lm} = 2\mu_s \langle \bar{\chi}^{lm} \rangle_s$ is a second order tensor.
$\langle K \rangle_f$	Permeability, a second order tensor. The i -th column is given by $\langle \mathbf{k}^i \rangle_f$.
k_{eff}	Isotropic permeability. Under symmetry, $k_{\text{eff}} = \langle \mathbf{k}_1^1 \rangle_f$
$\langle \cdot \rangle_f$	Volume average of a quantity over the melt portion of a cell, $\langle \cdot \rangle_f = \int_{Y_f} \cdot d\mathbf{y}$
$\langle \cdot \rangle_s$	Volume average of a quantity over the matrix portion of a cell, $\langle \cdot \rangle_s = \int_{Y_s} \cdot d\mathbf{y}$
P	Effective macroscopic (fluid) pressure, $P = p^{f(0)}$.
\mathbf{V}^f	Effective macroscopic fluid velocity, $\mathbf{V}^f = \langle \mathbf{v}^{f(0)} \rangle_f / \phi$.
\mathbf{V}^s	Effective macroscopic solid velocity, $\mathbf{V}^s = \mathbf{v}^{s(0)}$.
ζ_{eff}	Effective bulk viscosity of the matrix, $\zeta_{\text{eff}} = \mu_s \langle \zeta \rangle_s - \frac{2}{3}\mu_s(1 - \phi)$

Table 6. Notation for cell problems.

Symbol	Meaning
$\bar{\chi}^{lm}$	Velocity of the cell problem for a unit shear stress forcing on the solid in the lm component of the stress tensor
\mathbf{e}_i	Unit vector in the i -th coordinate, $\mathbf{e}_1^T = (1, 0, 0)$
\mathbf{k}^i	Velocity of the cell problem for a unit forcing on the fluid in the \mathbf{e}_i direction
$\bar{\xi}$	Velocity of the cell problem for a unit forcing on the divergence equation
π^{lm}	Pressure of the cell problem for a unit shear stress forcing on the solid in the lm component of the the stress tensor
q_i	Pressure of the cell problem for a unit forcing on the fluid in the \mathbf{e}_i direction
ζ	Pressure of the cell problem for a unit forcing on the divergence equation

Table 7. Additional notation for the other models.

Symbol	Meaning
C_0	An $O(1)$ Constant
κ	Permeability
κ_0	Permeability constant for a power law permeability, $\kappa = \kappa_0 \phi^n$
ζ_s	Bulk viscosity